

## BACHELOR

### A feedback control for the Flat Plank Tyre Tester

van Ballegooijen, M.J.J.

*Award date:*  
2006

[Link to publication](#)

#### **Disclaimer**

This document contains a student thesis (bachelor's or master's), as authored by a student at Eindhoven University of Technology. Student theses are made available in the TU/e repository upon obtaining the required degree. The grade received is not published on the document as presented in the repository. The required complexity or quality of research of student theses may vary by program, and the required minimum study period may vary in duration.

#### **General rights**

Copyright and moral rights for the publications made accessible in the public portal are retained by the authors and/or other copyright owners and it is a condition of accessing publications that users recognise and abide by the legal requirements associated with these rights.

- Users may download and print one copy of any publication from the public portal for the purpose of private study or research.
- You may not further distribute the material or use it for any profit-making activity or commercial gain

# **A feedback control for the Flat Plank Tyre Tester**

**M.J.J. van Ballegooijen**

**DCT 2006.100**

Bachelor's thesis

Coach: dr. ir. A.J.C. Schmeitz

Supervisor: prof. dr. H. Nijmeijer

Technische Universiteit Eindhoven  
Department Mechanical Engineering  
Dynamics and Control Technology Group

Eindhoven, October, 2006



## Abstract

An important issue in the tyre dynamics of motorcycles is the existence of camber sweeps during cornering. During such a camber-sweep, the motor cycle "sweeps" from one side to the other and the angle between the tyre and the road changes significantly.

Measurements with cambered tyres are executed on the Flat Plank Tyre Tester of the Eindhoven University of Technology. However, it is currently only possible to do tests with static camber angles.

The aim of this thesis is to design a feedback control system for the actuator of the Flat Plank Tyre Tester that drives the camber motion. This control makes it possible to execute tests on tyres with camber sweeps. For this purpose, first a mathematical model of tyre dynamics and experiments with camber sweeps executed by the University of Padova and TNO are considered. Then the current setup of the Tyre Tester and its possibilities are investigated and compared with the other experiments. Hereto, a kinematic relation between the angular velocity of the plank and the speed of the actuator is developed. From this, it follows that the present actuator on the test stand does not comply to the set demands, especially the angular velocity of the plank, which is driven by the actuator, is a problem.

On basis of the mathematical model and the measurements of Padova and TNO, demands for a new actuator are set. Based on these demands, a linear actuator of the CAP32-series from SKF with a D24CW motor with gear one is chosen.

After some calibrating and investigating measurements and the installation of the actuator on the Flat Plank, a Bode plot is obtained from the frequency response data of the actuator.

First, a simple proportional gain is tried for the feedback control. From this, the conclusion is drawn that a gain of 25 satisfies. This control is tested for six specific cases, based on the before mentioned experiments and mathematical model. For each experiment, the case with the lowest and the highest frequency is chosen. It follows that the maximum average relative error is 4.34% and the maximum absolute error  $0.767^\circ$ . The feedback control is implemented in a Simulink model.

Five of the six cases are executed on the Flat Plank with a motorcycle tyre while the plank has a forward velocity. The results of these measurements are compared with the results of the experiments of the other departments. The results did not quite match. It follows that it is hard to draw a conclusion from this, because more variables than the camber sweep and forward velocity of the plank are involved when studying the forces acting on a tyre during cambering. Therefore, it is recommended to do more research with regard to this topic.



## Samenvatting

Een belangrijke rol in de banddynamica van motoren speelt de aanwezigheid van zogenaamde camber sweeps tijdens het nemen van bochten. Tijdens een dergelijke camber sweep wordt een beweging beschreven waarbij de motor van de ene naar de andere kant helt. Hierbij verandert de hoek tussen het wegdek en de motor significant.

Metingen met hellende banden worden uitgevoerd op de Flat Plank Tyre Tester van de Technische Universiteit van Eindhoven. Echter, het is slechts mogelijk om experimenten te doen met statische hellingshoeken.

Het doel van dit verslag is het ontwerpen van een regeling met positieterugkoppeling voor de actuator die de hellingshoek van de plank aanstuurt. Deze regeling maakt het mogelijk om experimenten met bewegende hellingshoeken uit te voeren. Hiervoor is eerst gekeken naar een wiskundig model van de banddynamica en experimenten die gedaan zijn door de Universiteit van Padua en TNO. Hierna zijn de huidige opstelling en mogelijkheden bestudeerd en vergeleken met die andere experimenten. Daarom is eerst de kinematische relatie tussen de hoeksnelheid van de plank en de snelheid van de actuator opgesteld. Hieruit volgde dat de huidige actuator niet kan voldoen aan de gestelde eisen. Vooral de hoeksnelheid van de plank, die wordt aangestuurd door de actuator, is een probleem.

Aan de hand van het kinematisch model en de metingen van Padua en TNO zijn eisen opgesteld voor een nieuwe actuator. Uiteindelijk blijkt een lineaire actuator van SKF van het type CAP32 met een D24CW gelijkstroombmotor de beste optie te zijn.

Na enkele kalibratie en oriënterende metingen en de installatie van de actuator op de Flat Plank, is een Bode plot ontwikkeld uit de frequentie responsie data van de actuator. Eerst wordt ter oriëntatie een proportionele regelaar gemaakt met een waarde van 25. Dit blijkt al voldoende te zijn om aan de eisen te voldoen. Deze regeling is getest voor zes specifieke gevallen, die bepaald zijn uit het wiskundige model en de experimenten van Padua en TNO. Voor elk experiment zijn de gevallen met de laagste en de hoogste snelheid gekozen. Hieruit blijkt dat de maximale gemiddelde absolute relative fout 4.34% is en de maximale absolute fout  $0.767^\circ$ . Vervolgens is de regeling geïmplementeerd in Simulink.

Vijf van de zes experimenten worden uitgevoerd met een motorband terwijl de plank transleert. De resultaten van deze metingen worden vergeleken met de bijbehorende meting van de andere instanties. De resultaten kwamen niet overeen. Het is moeilijk om een conclusie te trekken uit de vergelijkingen, omdat meer parameters dan alleen de amplitude en de frequentie van de camber sweep invloed hebben op de krachten die op de band staan tijdens het camberen. Daarom wordt aanbevolen om met betrekking tot dit onderwerp meer onderzoek te doen.



# Contents

<b>I</b>	<b>Introduction</b>	<b>I</b>
1.1	Background . . . . .	1
1.2	Aim and scope . . . . .	1
1.3	Contents of this thesis . . . . .	1
<b>2</b>	<b>Camber dynamics</b>	<b>3</b>
2.1	Pacejka's model . . . . .	3
2.2	University of Padova . . . . .	5
2.3	TNO . . . . .	7
<b>3</b>	<b>Flat Plank Tyre Tester</b>	<b>9</b>
3.1	Present possibilities . . . . .	9
3.2	Kinematic relations . . . . .	10
3.3	Desired possibilities . . . . .	11
3.4	Demands vs. possibilities . . . . .	13
<b>4</b>	<b>Drive</b>	<b>15</b>
4.1	DC motor vs. actuator . . . . .	15
4.2	Desired specifications . . . . .	15
4.3	Comparison of actuators . . . . .	16
<b>5</b>	<b>Control of actuator</b>	<b>19</b>
5.1	Connection of the actuator . . . . .	19
5.2	Frequency response of the Flat Plank . . . . .	21
5.3	Feedback control . . . . .	21
5.4	Simulink model . . . . .	22
<b>6</b>	<b>Measurements with camber sweeps</b>	<b>25</b>
6.1	Measurements . . . . .	25
6.2	Results and comparison . . . . .	25
<b>7</b>	<b>Conclusions and recommendations</b>	<b>29</b>
<b>A</b>	<b>Effect of the non-lagging part ratio</b>	<b>31</b>
<b>B</b>	<b>Results of measurements on the flat plank</b>	<b>33</b>
<b>C</b>	<b>Information about the CAP/CAR32-series</b>	<b>35</b>
<b>D</b>	<b>Dynamic model</b>	<b>41</b>
<b>E</b>	<b>Manual of the intermediate device</b>	<b>43</b>
E.1	The connection of the actuator . . . . .	43
E.2	Driving the actuator . . . . .	43
E.3	Safety switch . . . . .	44
E.4	Manual Maxon current regulator . . . . .	45
<b>F</b>	<b>Measurements with the new actuator</b>	<b>49</b>
F.1	Without Flat Plank . . . . .	49
F.2	On the plank . . . . .	50
<b>G</b>	<b>Calibration of the actuator</b>	<b>53</b>
<b>H</b>	<b>Frequency response</b>	<b>55</b>





## List of symbols

$a$	[m]	length of the torsion-arm
$A$	[°]	amplitude
$A_r$	[rad]	amplitude
$b$	[m]	distance between upper shaft and point of fixation of the actuator
$d$	[m]	length of the actuator
$\dot{d}$	[m/s]	speed of the actuator
$\dot{d}_v$	[V/s]	speed of the actuator
$f$	[cycles/m]	camber sweep frequency
$f_c$	[-]	coefficient of friction
$F$	[N]	force
$F_{act}$	[N]	force exerted by the actuator
$F_y$	[N]	side force of the tyre
$F_z$	[N]	vertical force of the tyre
$h$	[m]	height
$J$	[kg · m <sup>2</sup> ]	mass moment of inertia
$K_y$	[N]	side force of the measuring hub
$K_z$	[N]	vertical force of the measuring hub
$m$	[kg]	mass
$M$	[Nm]	moment
$r$	[m]	distance from the point of action of a force
$r_s$	[m]	radius
$V$	[V]	feedback signal of the position
$V_L$	[V]	output voltage of the laptop sent to the TUeDACS
$V_{plank}$	[m/s]	forward velocity of the plank
$V_x$	[m/s]	forward velocity of the tyre
$w$	[m]	width
$x$	[m]	distance
$\beta_x$	[rad]	road camber angle
$\gamma$	[rad]	camber angle
$\gamma_L$	[rad]	lagging camber angle
$\gamma_{NL}$	[rad]	non-lagging camber angle
$\delta$	[rad]	angle of the plank
$\dot{\delta}$	[rad/s]	angular velocity of the plank
$\ddot{\delta}$	[rad/s <sup>2</sup> ]	angular acceleration of the plank
$\delta_{ini}$	[rad]	initial angle between $a$ and $b$
$\delta_t$	[rad]	angle between $a$ and $b$
$\varepsilon_{NL}$	[-]	non-lagging part ratio
$\omega$	[rad/s]	frequency



# 1 Introduction

## 1.1 Background

Since tyres of motorcycles deal with other circumstances than tyres of cars, the forces they both undergo differ much from each other. An important difference is that a car tyre is positioned almost perpendicular with respect to the road, while a motorcycle tyre often encounters so-called camber-sweeps. During such a camber-sweep, the motor cycle "sweeps" from one side to the other, which always occurs during cornering, and the angle between the tyre and the road changes significantly. Because this behavior is very important for the vehicle dynamics, several tyre models to describe this behavior and some setups on which experiments on tyres can be executed have been developed. Usually, such test stand can simulate the movement of a motorcycle tyre during cornering by rolling the tyre on a base, with the possibility to rotate the tyre around two axes to adjust both the steering angle and the camber angle. To simulate real conditions, it is necessary that the tyre can follow some prescribed trajectory. The University of Padova in Italy has such a tyre tester and has done a lot of experiments with camber-sweeps of motorcycle tyres.

The Automotive Engineering Science Laboratory of the Eindhoven University of Technology has another motorcycle tyre tester, called the Flat Plank Tyre Tester. This setup consists of a plank that can translate along its longitudinal axis and rotate around the same axis. Further, a tyre can be mounted on a base, which can translate vertically from and to the plank and rotate around the axis perpendicular to the plank, see figure 1.

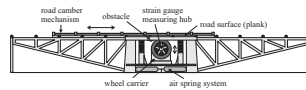


Figure 1: Overview of the Flat Plank Tyre Tester

## 1.2 Aim and scope

The present possibilities of the Flat Plank are not sufficient to execute camber sweep experiments. Currently, all movements of the test stand are driven by electric motors, which are not controlled by feedback systems. This is a problem, especially for the actuator that drives the rotational movement of the plank. It is possible to set a camber angle with this actuator, but camber sweeps are not feasible. The aim of this thesis is to develop a feedback control system for the linear actuator of the plank which makes it possible that the plank can follow a trajectory. For this purpose, demands for the actuation system are formulated, to check whether the required demands can be fulfilled with the current actuator. From this, it follows that it was better to buy a new actuator. Finally, the feedback controller is designed and tested.

## 1.3 Contents of this thesis

This thesis starts with discussing the relevant tyre dynamics in chapter two. The Flat Plank Tyre Tester of the University of Eindhoven and its current possibilities and kinematics are explained in the third chapter. Furthermore, the desired possibilities of the tyre tester are examined at the end of this chapter. In the fourth chapter, the possible drives for the tyre tester are compared and a satisfying drive is chosen, after all specifications are formulated. The design of the feedback control for the chosen actuator is discussed in chapter five. With a working feedback control, several measurements on a tyre are executed. The results of these experiments are discussed in chapter six. Finally, conclusions and recommendations are formulated in chapter 7.



## 2 Camber dynamics

The forces acting on a motorcycle tyre during a camber sweep depend on many parameters, like the sweep frequency, the angle amplitude and the vertical force due to the motorcycle and its rider. Some research has been performed, which is discussed here. Hans B. Pacejka [1] has investigated the dynamic behavior of tyres. Though most of his models are based on tyres of cars, they are in general also very useful for studying the behavior of motorcycle tyres. Furthermore, only TNO -the Dutch abbreviation of Dutch association for applied scientific research- and two universities have facilities do tyre tests with camber sweeps: the University of Padova and the Eindhoven University of Technology.

### 2.1 Pacejka's model

The mathematical model used for this thesis to describe tyre dynamics, is a model based on the findings of Hans B. Pacejka, found in his book "Tyre and vehicle dynamics" [1]. The force of interest in this thesis is the side force, exerted by the motorcycle tyre on the road. A look at the special case when the tyre is cambered is taken. Two of the parameters the side force  $F_y$  -figure 2- depends on, are the applied camber angle  $\gamma$  and the normal wheel load  $F_z$ .

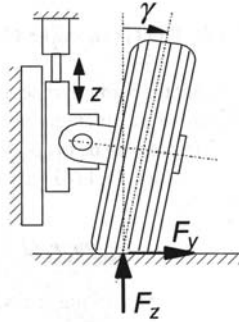


Figure 2: The side force  $F_y$ , the tyre normal load  $F_z$  and the camber angle  $\gamma$  [1]

The side force consists theoretically of two parts: a side force that is developed directly after the tyre is cambered and a side force that increases with increasing traveled distance. The instantaneous force is the so-called non-lagging force and is shown in figure 3 at a distance  $x=0$ . The non-lagging force appears in this case to act in the opposite direction of the steady-state side force, but there are also executed experiments where an equal direction has been reported.

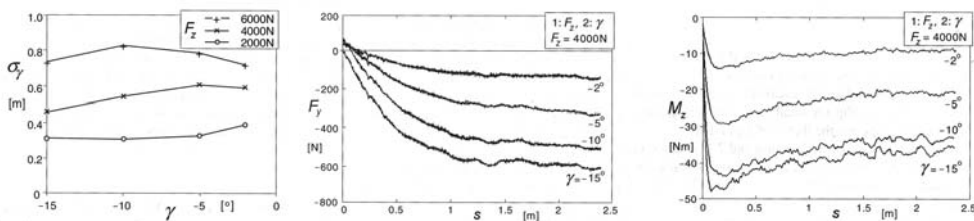


Figure 3: The relaxation length for step responses to different camber angles at various tyre loads, the side force response to step change in camber angle and the moment response to step change in camber angle (camber after loading [1])

The size of the non-lagging force depends on the order of the introduction of the load and the camber angle: a tyre which is first subjected to a camber angle and then moved to the road in normal direction appears to have a somewhat larger non-lagging force. Figure 4 gives the percentages of the non-lagging part with respect to the steady-state side force for different tyre loads and for the two considered ways of reaching the loaded and cambered condition before rolling has started. The tyre with the higher load appears to generate equally directed initial and steady-state side force responses to a change in camber angle. This tyre property can be implemented in the model by defining a non-lagging ratio  $\varepsilon_{NL}$ , which is the proportion of the input camber angle  $\gamma_{NL}$  and the camber angle  $\gamma$ . Hereby causes the  $\gamma_{NL}$  the non-lagging response  $\varepsilon_{NL} \cdot \gamma$  and yields the remaining part  $\gamma_L$  the lagged response  $(1-\varepsilon_{NL}) \cdot \gamma$ .

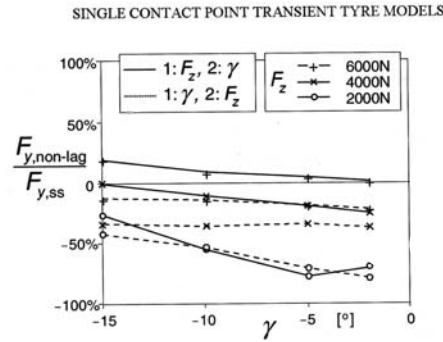


Figure 4: Non-lagging part of side force response for the cases (1) applying camber after having loaded the tyre and (2) loading the tyre normal to the road after having cambered the tyre without load [1]

Pacejka's model has been implemented in a mathematical model, which calculates by means of specific given parameters the lagging and non-lagging forces. In this computer model, the following important parameters can be substituted:

Table 1: Used parameters in the mathematical model

Parameters	Value
Contact patch mass [kg]	1
Sidewall stiffness [N/m]	$10^5$
Sidewall damping [Ns/m]	2000
Relaxation length [m]	0.02
Forward velocity [m/s]	$4.75 \cdot 10^{-2}$
Vertical load [N]	1475
Non-lagging part ratio [-]	0.5
Camber stiffness [N/rad]	$1475 \cdot 0.98$
Wheel moment of inertia [ $kgm^2$ ]	1
Camber angle amplitude [deg]	15
Sine sweep frequency [rad/s]	0.05

Most of these parameters depend on tyre properties, like the relaxation length and the sidewall stiffness and damping. Other parameters can be adjusted to the circumstances of the experiment, like the forward velocity, the vertical load and the camber angle amplitude. Furthermore, the way the camber angle is applied can be chosen: by a step change in de camber angle or by a sine wave. From these data, the lagging and the non-lagging parts of the lateral force and the difference between them are calculated and plotted against distance.

The scope of the executed experiments on the Tyre Tester is to investigate the lagging behavior of the

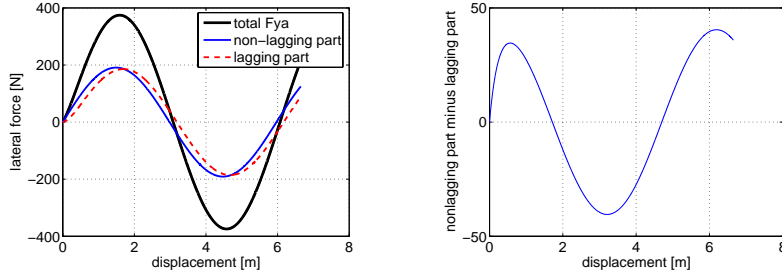


Figure 5: Lateral forces plotted against distance with the data obtained from table 1 (1) and the difference between the lagging and non-lagging force  $r$

lateral force  $F_y$ . This means that the parameters must be adjusted, so that the simulation shows a clear lagging of  $F_y$ , i.e. the difference between the non-lagging and the lagging forces is clearly noticeable. This is, because the lag of  $F_y$  depends on the theoretical lagging force.

The contribution of the non-lagging part in comparison with the lagging part depends on the sine sweep frequency: a low frequency should cause a high contribution of the lagging force with no noticeable influence of the non-lagging force. Conversely, a very high frequency should cause a high contribution of the non-lagging part with a very low lagging part, [1]. However, the contributions of both the lagging and the non-lagging part depend also on the non-lagging part ratio  $\varepsilon_{NL}$ : the lagging force will never exceed the lagging force with an  $\varepsilon_{NL}$  higher than 0.5, see figures 29 in appendix A. For the concerned tyre, the ratio has been determined with several measurements [2]. The ratio depends on the circumstances of the measurements and is approximated to be 0.5 for the considered motorcycle tyre, which means that the lagging force will never exceed the non-lagging force, no matter what sine sweep frequency or forward velocity.

Furthermore, the lagging part is dependent on the traveled distance with an applied camber angle  $\gamma$  combined with the relaxation length  $\sigma$ .

When the parameters of table 1, with an amplitude of  $15^\circ$  and a sine sweep frequency of 0.05 rad/s, are taken, a clear difference between the lagging and non-lagging forces is noticeable, see figure 5. This case corresponds to a path frequency of 0.168 cycles per meter.

## 2.2 University of Padova

The University of Padova has performed a lot of so-called quasi-static tests on tyres during camber sweeps. The tests are quasi-static because the sweep frequency and the forward velocity of the tyre are very low. The setup on which these experiments are executed, consists of a tyre that rolls over a rotating circular road, see figure 6.

The University of Padova tested two different tyres: a slick front tyre for racing motorcycles with an inflation pressure of 2.5 bar which encountered a vertical load of 900 N and a scooter front tyre with the same inflation pressure and an applied vertical load of 1570 N. During these tests, the phase angle between the camber motion and the measured lateral force  $F_y$  was calculated. The executed tests on the tyre were different. The slick front tyre was tested with a camber sweep amplitude of  $1^\circ$ , while the path frequencies changed: the angular speed of the rotating disc varied from 1-16 km/h and the frequency of the camber sweep varied from 0.05-0.5 Hz. Both the angular speed and the camber sweep frequency did not change during the test itself. These velocities and frequencies lead to path frequencies in the range 0.01-0.75 cycles per meter. The resultant phase angle is plotted against the path frequency in figure 7.

The most noticeable result of this experiment is the existence of negative phase angles when the path frequency is higher than 0.05 cycles per meter. This means that the camber force leads the camber motion. The experiments executed on the scooter tyre were different from the slick tyre; a smaller range of path frequencies was considered. The range was taken between 0.01 and 0.1 cycles per



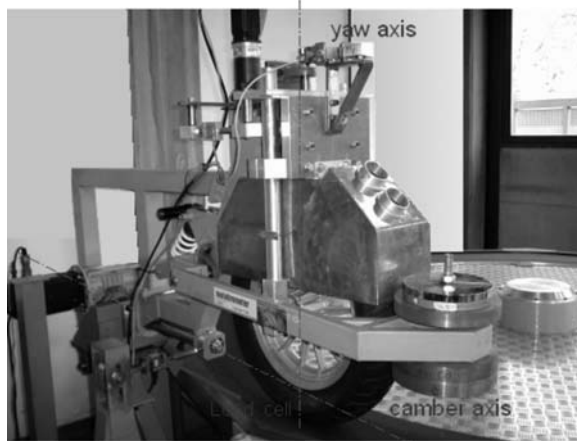


Figure 6: The tyre tester of the University of Padova [3]

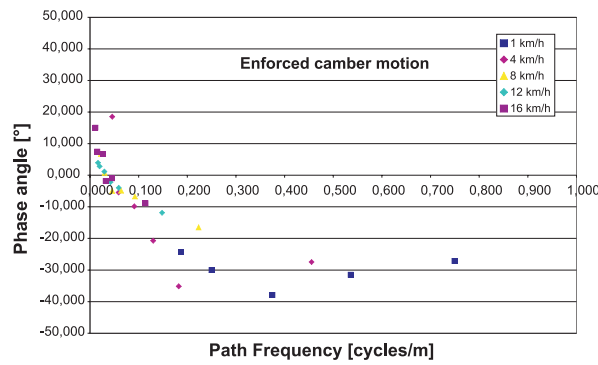


Figure 7: The phase angle plotted against the path frequency for the slick tyre [3]

meter. The range of speed was 2-12 km/h and the frequency of the motion 0.006-0.333 Hz. Also a higher camber sweep amplitude was set: one test was executed with an amplitude of  $5^\circ$ , the second with  $10^\circ$  and one test with an applied amplitude of  $20^\circ$ . The results of these experiments are put together in figure 8.

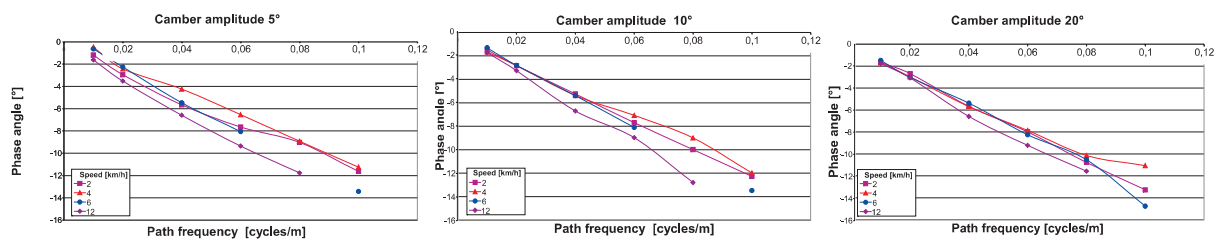


Figure 8: The phase angle plotted against the path frequency for the scooter tyre for different camber amplitudes [3]

In this case, the phase angle is always negative; the camber force leads the camber motion.

## 2.3 TNO

TNO has a vehicle in which a tyre can be appended, so that the tyre experiences the forces of the road during cornering while the vehicle moves. In this way, the circumstances during a camber sweep are almost the same as on a motorcycle. The vehicle moves with a velocity of 60 km/h and the tyre undergoes sweeps of 5, 15 and 25 degrees per second. This is 0.3, 0.9 and 1.5 degrees per meter respectively. These parameters match the angular velocities of camber sweeps of motorcycles. The results of the experiments done on the Flat Plank Tyre Tester in Eindhoven are compared with the results of the two above mentioned experiments. The Flat Plank is discussed in the next chapter. The circumstances of the camber sweeps, like forward velocity and sweep frequency, are converted into the demands of the Flat Plank.



### 3 Flat Plank Tyre Tester

The Automotive Engineering Science Laboratory has the Flat Plank Tyre Tester since 2003. The original setup consists of a 7 m long plank that can translate about 7 m along its longitudinal axis with a minimum speed of 0.02 m/s and a maximum speed of 0.0475 m/s. Further, a tyre can be mounted on a carrier which can apply a vertical load on the tyre by translating vertically from and to the plank and rotate around the axis perpendicular to the plank to apply a steering angle (figure 9). As can be seen in the figure, the wheel carrier is beneath the plank, so it is the reverse of the normal situation.



Figure 9: Overview of the Flat Plank Tyre Tester

#### 3.1 Present possibilities

After a few years, the setup was adapted in such way that the demand for a rotating plank could be fulfilled. To be able to rotate the plank, the plank was mounted on a shaft by horizontal and vertical bars, while it rotates around another, lower, shaft. A linear actuator is attached to another bar, the so-called torsion-arm, which is fixed to the upper shaft, see figure 10. After this adaptation, experiments with road camber angles can be executed.

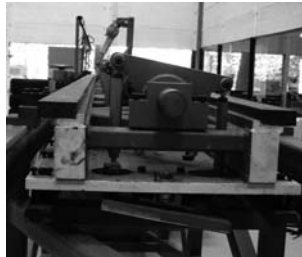


Figure 10: Close-up of the road camber rotation mechanism of the Tyre Tester

The actuator that drives the rotational movement of the plank, is a CAR32 type, produced by SKF. It is driven by a 24V DC motor. The maximum stroke of this actuator is 0.100 m, with a minimum speed of 0.010 m/s and a maximum speed of 0.015 m/s. It can supply a maximum force of 3500 N, in both inward and outward direction. The actuator is operated by a potentiometer with one knob to set the velocity of the actuator and two buttons to set the stroke of the actuator. The speed of the actuator depends on the incoming voltage of the DC motor, which is determined by the knob of the potentiometer. However, the force exerted by the DC motor on the Flat Plank also indirectly depends on this voltage. So, when the set voltage is too low, the exerted force is too low and the plank will not move.

With this setup, it is possible to measure the forces and moments acting on the motorcycle tyre during rolling with a camber angle. However, all tunings needs to be done manually, because there is no feedback control implemented in one of the electric motors and their controls. Examples of tunings are the steering angle of the tyre, the normal force of the tyre exerted on the plank and of course the

camber angle. When for example a certain camber angle is desired, the angle of the plank has to be measured manually with a digital clinometer, to know when the plank has the desired angle and the rotation must be stopped. This means that it is only possible to execute static test, except the horizontal movement of the plank. However, this does not match reality.

It is clear that it is necessary to perform dynamic tests to match reality. Because a motorcycle often experiences camber sweeps, the plank has to be able to perform a rotation following a prescribed path.

### 3.2 Kinematic relations

First, it is important to know what the kinematic relations are between the actuator and the tyre tester when the plank rotates according to a prescribed path. Hereto, a cross section of the tyre tester has been made, see figure 11. Because the plank is not directly driven by the actuator, it is important to point out the connection between the translation of the actuator and the rotation of the plank. Some measurements of the stroke of the actuator and the corresponding angle, with respect to the horizontal, of the actuator itself and the plank, have been carried out. Besides this, the angle of the torsion-arm has been measured for the determination of the rotation of the upper shaft. The results are shown in table 5 in appendix B.

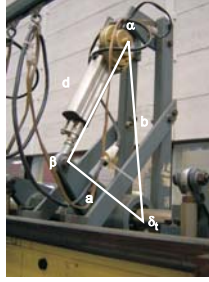


Figure 11: Close-up of the actuator

From this, the conclusion that the rotation of the upper shaft corresponds linearly to the rotation of the plank is drawn; there is no gear between them. Later, this has also been validated experimentally, see appendix G

To know the exact relation between the stroke of the actuator and the rotation of the plank, a kinematic model is formulated. Therefore, the above mentioned mechanism is simplified to a triangle: the first corner,  $\alpha$ , is the point of rotation between the actuator and the setup, corner  $\beta$  is the point of rotation between the actuator and the torsion-arm and corner  $\delta_t$  is the point of rotation of the upper shaft. This last point is important because with the change of  $\delta_t$  in time, the angular velocity of the upper shaft and so the angular velocity of the plank can be determined. Furthermore, the length of two sides of the triangle are known, namely the distance between points  $\beta$  and  $\delta_t$  and the distance between  $\alpha$  and  $\delta_t$ . The distance between  $\alpha$  and  $\beta$  is the length of the actuator, which changes. With these parameters, the relation between the three sides and the angle  $\delta_t$  is known. This relation can be determined with help of the cosine rule:

$$d^2 = a^2 + b^2 - 2 \cdot a \cdot b \cdot \cos(\delta_t) \quad (1)$$

with  $a$  and  $b$  the known sides, namely 0.175m resp 0.443m.  $\delta_t$  consists of two angles: the angle of the plank  $\delta$  and the initial angle  $\delta_{ini}$  between  $a$  and  $b$ , 1.15 rad. This relation is plotted in figure 12, which is almost linear for the range studied.

Also the speed of the actuator is studied. Though it was not a very precise measurement, it surely is useful for e.g. comparison with other experimental adjustments, which will be later examined. During this measurement, the time it takes for the actuator to fully move out and in with different adjustments of the potentiometer is measured. The results are mentioned in table 6 in appendix G. The minimum speed of the actuator is 7.69 mm/s and the maximum speed is 16.7 mm/s.

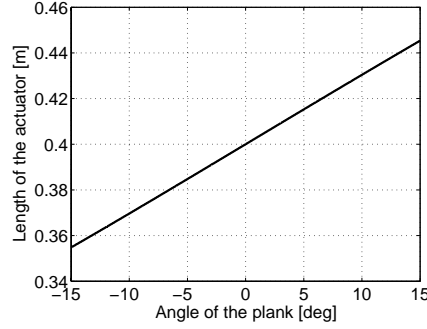


Figure 12: Close-up of the actuator

### 3.3 Desired possibilities

The results of the experiments executed on the Flat Plank Tyre Tester will be compared with the mathematical model of Pacejka, the results of the University of Padova and the experiments of TNO. So these experiments determine the demands of the Flat Plank Tyre Tester and the actuator for the camber angle in particular.

In formulating the demands of the Flat Plank, the minimum and maximum angular velocity of the plank, and so the corresponding velocities of the actuator, are most interesting.

When the derivative of equation 1 is taken, with

$$\delta_t = A \cdot \sin(2 \cdot \pi \cdot f \cdot x) + \delta_{ini} \quad (2)$$

the relation between the velocity of the actuator [m/m] and the angular velocity of the plank, in  $^\circ/\text{m}$  can be set up:

$$\frac{d\delta}{dx} = \frac{2 \cdot a \cdot b \cdot \frac{d\delta}{dx} \cdot \sin(\delta)}{\sqrt{a^2 + b^2 - 2 \cdot a \cdot b \cdot \cos(\delta)}} \quad (3)$$

with

$$\frac{d\delta}{dx} = A \cdot 2 \cdot \pi \cdot f \cdot \cos(2 \cdot \pi \cdot f \cdot x) \quad (4)$$

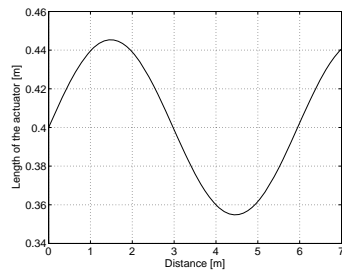
with  $A$  the camber amplitude [ $^\circ$ ] and  $f$  the camber sweep frequency [cycles/m].

As mentioned before, the forward velocity of the plank lies between 0.02 m/s and 0.0475 m/s and a maximum camber angle of 15 $^\circ$  can be accomplished.

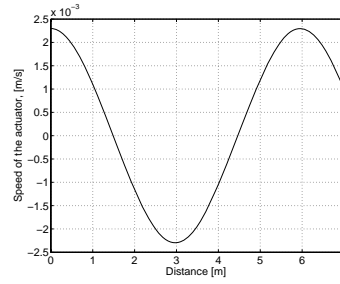
First, the mathematical model of Pacejka is considered. In chapter 2.1, with a path frequency of 0.168 cycles/m, a clear distinguish between the non-lagging and lagging forces can be made. The minimum angular velocity -with an amplitude of 15 $^\circ$ - is infinitesimal small, following from equation 3; it is not possible to calculate the exact value for the minimum velocity. To make an estimate for the minimum velocity, the mean velocity is taken. From figure 13(a) can be determined that it takes about 1.5 m to move 0.045 m. The mean velocity is 0.03 m/m. With the minimum forward velocity of 0.02 m/s, the minimum velocity is 0.6 mm/s. The maximum angular velocity is, with a forward velocity of the plank of 0.0475 m/s and the same amplitude and path frequency, 2.30 mm/s and can be derived from figure 13(b).

The angular velocities of the Flat Plank to meet the conditions of the tests in Padova are calculated likewise. The lowest path frequency of the tests is 0.01 cycles per meter and the lowest amplitude 5 $^\circ$ , the highest path frequency 0.1 and the highest amplitude was set to 20 $^\circ$ . Since this is beyond the range of the Flat Plank, an amplitude of 10 $^\circ$  is taken, because the test results of these parameters are known. The minimum velocity of the actuator is 0.0174 mm/s (figure 14(a)) and the maximum velocity 1.37 mm/s, figure 14(b).

The camber sweep amplitudes and frequencies of the tests executed by TNO are unknown. Only constant velocities are known, which are 0.3, 0.9 and 1.5 $^\circ/\text{m}$ . Because the test dealt with camber sweeps,

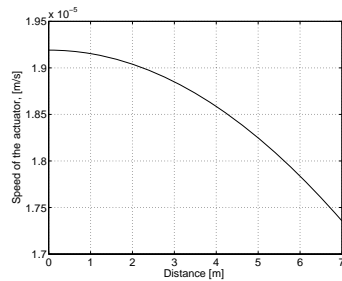


(a) The length of the actuator for  $v=0.02$  m/s,  $A=15^\circ$  and  $f=0.168$  cycles/m

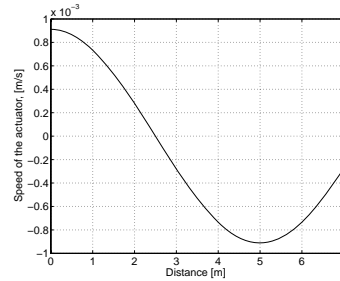


(b) The velocity of the actuator for  $v=0.0475$  m/s,  $A=15^\circ$  and  $f=0.168$  cycles/m

Figure 13: Pacejka



(a) The velocity of the actuator for  $v=0.02$  m/s,  $A=5^\circ$  and  $f=0.01$  cycles/m



(b) The velocity of the actuator for  $v=0.0475$  m/s,  $A=10^\circ$  and  $f=0.1$  cycles/m

Figure 14: Padova

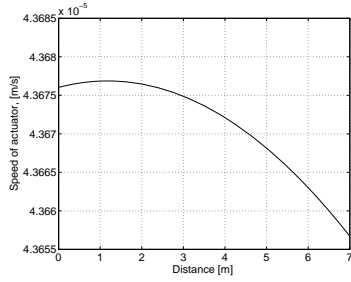
the assumption that the camber sweeps were not exactly sinusoidal but more sawtooth-like can be made. Tests with several amplitudes have been done, but as the Flat Plank has a maximum amplitude of  $15^\circ$ , the amplitude range will be taken as  $5^\circ$  to  $15^\circ$ . The resulting minimum and maximum angular velocity are  $0.006^\circ/s$  resp.  $0.0713^\circ/s$ , with a forward velocity of the plank of  $0.02$  m/s resp.  $0.0475$  m/s. But with an angular velocity of  $0.006^\circ/s$ , the plank almost does not move. Therefore, a forward velocity of the plank of  $0.0475$  m/s is taken, which leads to an angular velocity of  $0.0143^\circ/s$ . The corresponding velocities of the actuator are determined from the figures below and are  $0.0437$  mm/s and  $0.217$  mm/s.

An overview of the six considered cases and the following velocities of the actuator is included in table 2.

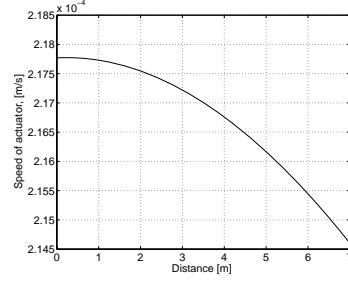
So, the desired demands of the flat plank are

- The possibility to let the plank follow a trajectory
- A minimum angular velocity of  $0.0174$  mm/s and a maximum angular velocity of  $2.30$  mm/s

However,  $0.0174$  mm/s means that the Flat Plank almost does not move. A required minimum angular velocity of  $0.217$  mm/s is more reasonable.



(a) The velocity of the actuator for  $v=0.02$  m/s and  $\dot{\delta}=0.006^\circ/s$



(b) The velocity of the actuator for  $v=0.0475$  m/s and  $\dot{\delta}=0.0713^\circ/s$

Figure 15: TNO

Table 2: The six cases considered

Case		Parameters		$V_{plank}$ [m/s]	Velocity [mm/s]
		Amplitude [°]	Path freq. [cycle /m]		
1	Math model of Pacejka	15	0.168	0.02	0.60
2	Math model of Pacejka	15	0.168	0.475	2.3
3	University of Padova	5	0.01	0.02	0.0174
4	University of Padova	10	0.1	0.0475	1.37
5	TNO		$0.0142^\circ/s$	0.02	0.0437
6	TNO		$0.0713^\circ/s$	0.0475	0.217

### 3.4 Demands vs. possibilities

As mentioned in the previous section, the minimum velocity of the present actuator in the current set up is 7.69 mm/s, which is too fast for the desired experiments. A current regulator might solve this problem. The outgoing current of this device can be set by the incoming voltage of the current regulator. This outgoing current is the incoming current of the DC motor. With this current regulator, it is possible to decrease the speed of the actuator without decreasing the force of the actuator. The regulator can be implemented in a control loop, and with a position sensor the displacement of the actuator can be fed back. Finally, by implementing above mentioned in a feedback control loop, the problem should have been solved.

However, the setup would be very sensitive because the current regulator really forces the actuator's DC motor to operate at a speed one fourth to one fortieth of the rated minimum speed. This would make the control loop very complex. Besides this, it would significant shorten the lifetime of the motor.

Also the possibility of a gear between the actuator and the plank could be considered, but as this would involve a lot of constructional problems and time, this is not the most convenient solution.

In conclusion it is better to purchase a new drive for the rotational movement of the plank.





## 4 Drive

As concluded in the preceding chapter, a new drive for the Flat Plank is needed. There are many ways to drive the Flat Plank. Examples are linear actuators driven by a DC motor, like the present actuator, or rotary actuators. The last one is logical, because the plank rotates. Both rotary and linear driving systems, driven in different ways like electric or hydraulic, are dealt with in this section.

### Rotary

Because a drive to rotate the plank is searched, a rotary drive would be very obvious. A disadvantage is, however, that the present construction is not built for a rotary drive. So, with a rotary drive, the present construction is useless and the setup needs to be adapted to a rotary drive, which involves constructional problems. Since time is spare, it is not the most advisable drive.

### Linear

With the rotary drive rejected, linear drives remain. Among these drives a range of possibilities exists, like pneumatic, hydraulic and electric. Although a hydraulic drive is very smooth, it is not desirable because it involves oil pumps and high costs. The same holds for pneumatic drives, in which air pressure instead of oil is needed. So, electric actuators remain, leaving combustion engines out of consideration. Within electric drives, the choice between AC and DC motors must be made. The present actuator has a DC motor, so the power supply for such motors is available. In conclusion, a linear actuator with a DC motor is the most appropriate choice.

Now that the choice for a linear actuator with a DC motor is made, it is likely to discuss whether it is possible to just purchase a new DC motor for the current actuator, instead of purchasing a whole new actuator. This, because the new actuator will be very similar to the present actuator. This choice is discussed in the next section.

#### 4.1 DC motor vs. actuator

As mentioned above, first the choice between purchasing a new actuator or only a new DC motor for the current actuator is made. The main advantage of a new DC motor is of course the costs; a new actuator would be less desirable from an economic point of view than a DC motor. Another profit is that the same actuator could be used, so there would be no chance of an ill-fitting actuator. On the other hand, the possibility that the DC motor does not fit on the current actuator exists, which would probably involve more problems than a non-fitting actuator. Furthermore, an encoder or potentiometer is needed for the feedback of the position of the actuator. This would involve constructional problems. Another important aspect in the choice between the motor and the actuator is that the Flat Plank Tyre Tester was occupied for a long time. A new actuator would sidestep this: the actuator and its feedback control could e.g. be tested on a tensile testing machine.

In the end, considering above mentioned, it is decided to buy a new actuator.

#### 4.2 Desired specifications

Now the choice for a new linear actuator has been made, the desired specifications of the actuator must be composed. The most important specifications are a speed range of 0.217-2.30 mm/s, see section 3.3, and the ability to give feedback of the position of the actuator. Furthermore, it is desirable that the new actuator has the same length as the old one, since the set-up has been designed to fit that actuator. The maximum force the actuator can exert could be important too, but it is rather difficult and time-consuming to calculate this force, so it is decided that the maximum force of the current actuator satisfies, because this force proved to be sufficient in the past. Of course, the new actuator must be able to exert the force in both inward and outward direction. The remaining specifications can be the same as the old actuator, because they satisfy.

The specifications are summarized in table 3.

Table 3: Specifications of both old and new actuator

Specs	Old actuator	New actuator
Rated voltage (V)	24	24
Rated current (A)	8	-
Rated speed (rpm)	5500	3500
Linear speed (mm/s)	10-15	0.217-2.30
Max dynamic force (N)	3500	3500
Brushlife (h)	1500	1500
Stroke (mm)	100	100
Initial length	218	218

### 4.3 Comparison of actuators

There are a lot of companies that offer actuators. Because the old actuator is delivered by SKF and the Eindhoven University of Technology is familiar with this company, information about actuators was gathered at SKF. SKF delivers many variations of actuators, but since an actuator similar to the old one is desirable, the possibilities within the CAR-series have been considered. The CAR-series is similar to the CAP-series, except for the potentiometer for the feedback signals integrated in the last one. In figure 16 graphs with the possible loads and corresponding velocities and currents of the considered actuators are displayed. More information about the CAR/CAP-series is given in appendix C.

Performance diagram

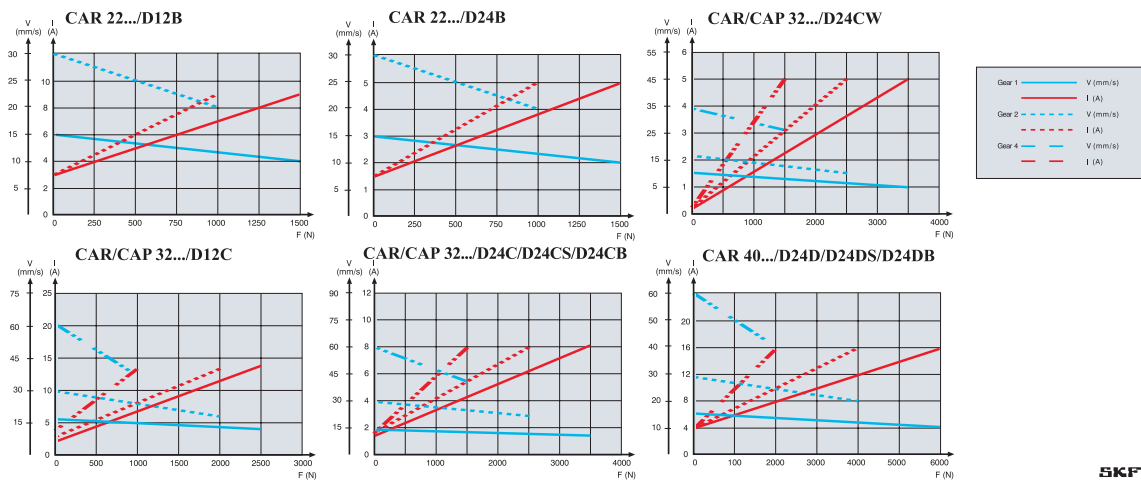


Figure 16: Overview of loads, velocities and currents of SKF actuators

From these graphs it is clear that the actuator of type CAP 32, with gear 1 and D24CW motor, complies best with the demands, though the velocity is still a problem. But since this is the only actuator with the lowest velocity, it is advised to take this. As mentioned before, the old actuator is of type CAR 32, with a D24D motor and gear 1.



## 5 Control of actuator

This chapter discusses the implementation of the new actuator at the Flat Plank and the required hardware and the design of the feedback control for this actuator. First, some test were executed on the actuator before it was mounted at the Flat Plank. After some tests on the Flat Plank, it turned out that a feedback control is needed. Hereto, first a dynamic model of the actuator and the Flat Plank has been set up, see appendix D. However, it turned out that the parameters required for this model are difficult to determine. In addition, the dynamics of the devices between the laptop and the actuator is unknown. Therefore, the required frequency response function of the Flat Plank is determined experimentally. Finally, the feedback control is developed and tested.

### 5.1 Connection of the actuator

Before the actuator was ready to be operated by laptop, all electronics between the laptop, the TUEdACS, the power supply of the actuator and the actuator itself are connected. A user-friendly intermediate device is made, on which the actuator and the TUEdACS with all their in- and output signals can easily be plugged in. This setup is shown in figure 17. More detailed figures and a manual for the connection of the three devices, the laptop and the actuator are found in appendix E.

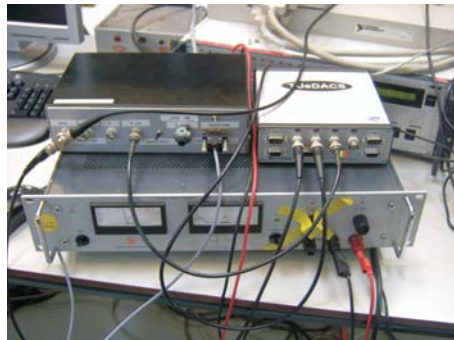


Figure 17: Overview of the electronics of the actuator. The lowest device is the power supply, on which on the right the TUEdACS and on the left the intermediate device is placed

When the actuator is operated from the the laptop, the desired signal, in Volt, is sent from Simulink in Matlab to the TUEdACS. The required model and software for the communication between the laptop and the TUEdACS run from a CD-ROM. The TUEdACS sends this signal via the intermediate device to the current regulator, which sends a current to the actuator. Further, the power supply of the actuator is connected to the intermediate device. The actuator sends three signals back: its stroke, the current intensity and the rotational speed of the motor. These signals are received by the intermediate device and send to the Simulink model via the TUEdACS. Because the TUEdACS has two inputs, only two signals can be send to the Simulink model. Furthermore, the actuator has two end switches which prevent the actuator to destroy itself by moving too far in or out. These are also connected to the intermediate device. When the actuator reaches an end switch, the actuator stops and can only move again, to the opposite side of course, after a safety switch is opened manually. It is important that the switch is not opened when the actuator moves in the direction of the end switch. The end switch will not have any use any more and the actuator may fail.

Before the actuator and all its electronics are mounted at the Flat Plank, the actuator is tested with only its hardware and electronics to check whether everything works properly and to find out how the actuator responds on signals given by a Simulink model in Matlab to the TUEdACS.

First, some calibrating measurements are done to obtain the relation between the feedback voltage, that is related to the stroke of the actuator, and the stroke measured in millimeters. Furthermore, the end switches are tested and calibrated, to know the real range of the stroke of the actuator. These tests made clear that the range of the actuator is  $0.068-4.074V$ , or  $0-102mm$ . Now, the conversion rate

between voltage and millimeters is known:  $1 \text{ V} \equiv 25.48 \text{ mm}$ . Also some tests with a constant output voltage, which gives a constant speed of the actuator, and a sine wave are executed. The results of these measurements are included in appendix F.1. The relation between the input voltage and the velocity of the actuator [V/s] is:

$$\dot{d} = 0.0851 \cdot V - 0.0022 \quad (5)$$

with a maximum velocity of the actuator  $0.168 \text{ V/s}$ , or  $4 \text{ mm/s}$ . It appears that the equilibrium value of the sinusoidal movement increases. The actuator's position during a sine wave with frequency  $5 \text{ rad/s}$  and an amplitude of  $1$  is shown in figure 18.

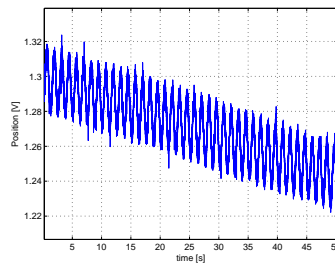


Figure 18: The position of the actuator in Volt during a sine wave with  $F=5 \text{ rad/s}$  and  $A=1$

After these tests the actuator was mounted at the Flat Plank. Again, some calibrating tests are executed to point out the relation between the angle of the plank and the stroke of the actuator, measured in Volt. Although a kinematic relation has been formulated, see chapter 3.2, a calibration can be very helpful to obtain a better accuracy. The relation between the angle of the plank and the stroke of the actuator can be approximated as linear, see figure 19, which was also concluded from section 3.2. The results of the measurements are included in appendix F.1.

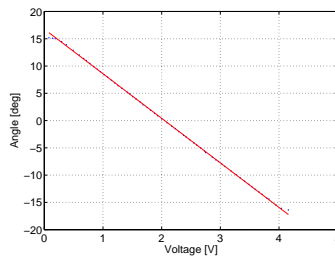


Figure 19: The measured voltage plotted against the measured angle of the plank (blue spots), with a straight line through it

Then the same tests are executed as before the implementation of the actuator in the Flat Plank. These results are included in appendix F.2. It appeared that the speed of the actuator is lower with the same constant. This is logical, because the actuator now exerts a force, in contradistinction to the former situation. The actuator behaves also differently at a sine wave. As shown in figure 20 the sine wave does not shift as much as in figure 18 but it still is not a pure sine wave. This might need to be compensated by the feedback control. Furthermore, the velocity of the actuator increases for an input voltage between  $0$  and  $3.5 \text{ V}$ ; after  $3.5 \text{ V}$  the velocity remains the same, no matter what voltage. With this setup, it appears that sine waves with amplitude  $15^\circ$  and frequency  $0.112 \text{ rad/s}$  or with amplitude  $1^\circ$  and frequency  $1.68 \text{ rad/s}$  are the limit, see appendix F.2. Any sine wave with a higher frequency in the first case or a larger amplitude in the second case can not be followed. The maximum velocity is  $1.68^\circ/\text{s}$ .

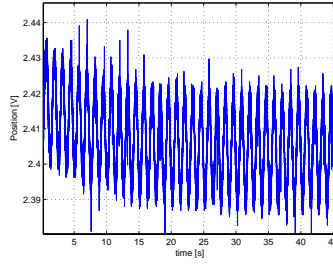


Figure 20: The position of the actuator on the plank in Volt during a sine wave with  $F=5$  rad/s and  $A=1$

## 5.2 Frequency response of the Flat Plank

For the design of the feedback control a Bode plot, obtained from the measurements of the frequency response of the Flat Plank, is drawn.

In order to measure the frequency response, sine waves with different frequencies are send to the actuator. From the feedback position signal the amplitude and the phase lag of the actuator are known. With this information a Bode plot is developed. The sine frequencies and the resulting amplitudes and phase lags of the actuator are gathered in table 10 in appendix H. To obtain the desired Bode plot, the frequency is plotted against the amplitude on a log scale and potted against the phase lag on a semi log scale. The resulting Bode plot is shown in figure 21. However, the following comment must be made: the input signal is a voltage which results in a velocity, while the output signal is a voltage, representing the position of the actuator. So, in fact the transfer between the input and output voltage is studied, in stead of the transfer between the reference and resulting position.

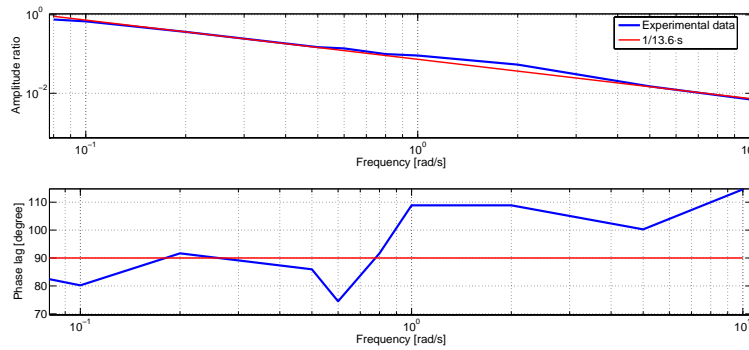


Figure 21: The Bode plot of the Flat Plank

## 5.3 Feedback control

With help of this Bode plot, a feedback control can be shaped. First, the transfer function  $H$  between the input and output voltage is derived from the Bode plot. Because the slope of the amplitude plot has magnitude  $-1$ ,  $H$  is described by  $\frac{1}{m \cdot j \cdot \omega}$ . The value of  $m$  can be derived by plotting a line that fits the amplitude plot. With  $m=13.6$ ,  $H$  comes closest to the amplitude plot, see the red line in figure 21. From this, the conclusion could be drawn that it is a first order system. However, as mentioned before, this concerns the transfer between a velocity and a resulting position. The Flat Plank itself, including the before mentioned devices, is a second order system when considering the transfer function of the positioning. But as in the end the velocity is taken as the input, the Bode plot of this first order system



will be used for the design of the feedback control.

Because the system is already stable for the interesting frequencies, first a proportional control is tried. This control is tested with several gains. It turns out that with a gain of 30 or higher, the actuator starts to oscillate with a very high frequency and low amplitude. This behavior is hardly noticeable from the position and amplitude feedback, but it truly is audible. An explanation could be the amplifying effect of the gain on the present noise, though the feedback signal is filtered. With a gain of 25, noise is less amplified and the actuator behaves more stable.

Of course, the gain must satisfy for all cases mentioned in chapter 2, so the control is tested for six cases: for each kind of investigation the case with the lowest and the highest angular velocity is studied. The results are put together in table 4.

Table 4: The maximum error and mean error for six cases

Case		Parameters		Mean relative error [%]	Maximum error [°]
		Amplitude (°)	Frequency (Hz)		
1	Mathematical model of Pacejka	15	$\frac{0.0250}{\pi}$	4.34	0.571
2	Mathematical model of Pacejka	15	$\frac{0.0250}{\pi}$	3.92	0.767
3	University of Padova	5	0.0002	0.77	0.5847
4	University of Padova	10	0.00475	1.93	0.5792
5	TNO		0.0142°/s	0.44	0.5883
6	TNO		0.0713°/s	1.74	0.5269

It appears that the gain satisfies for all these cases; the actuator follows the set trajectory with a small error.

## 5.4 Simulink model

The feedback control is implemented in a Simulink model, see figure 22. The model uses six parameters, obtained from an m-file, namely the camber sweep amplitude and frequency, the offset value of the sweep, the number of camber sweeps, the angular velocity and the initial position of the plank for the constant velocity. The first four parameters are used for camber sweeps, the last two for constant angular velocities of the plank.

The model contains three systems: figure 22a is the reference signal, figure 22b is the actual control and figure 22c is the stop function. In figure 22a, the choice between a sine wave and a constant velocity can be made by the left switch. The parameters of the sine wave are set by the m-file, as is the angular velocity. The second switch can be used to set the initial position of the plank. The signal obtained from the sine wave, the angular velocity or the initial position is calculated in degrees, which must be converted into a voltage. The determination of the conversion ratio is included in appendix G.

Figure 22b is a regular feedback control. It contains the previous mentioned reference signal, the gain and a saturation block to chop outgoing signals higher than 10 or lower than -10 V off. This signal leaves through the ToTUEdACS-block, to the TUEdACS. The feedback signal enters through the FromTUEdACS-block and is subtracted from the reference signal, resulting in the error signal.

The stop function stops the measurement after a specific time, obtained from the division of the desired number of sweeps by the sweep frequency, set in the m-file.

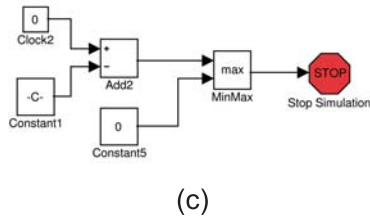
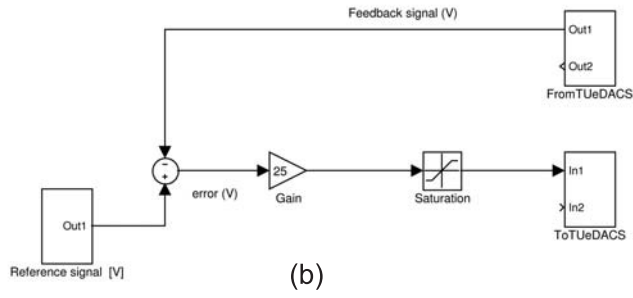
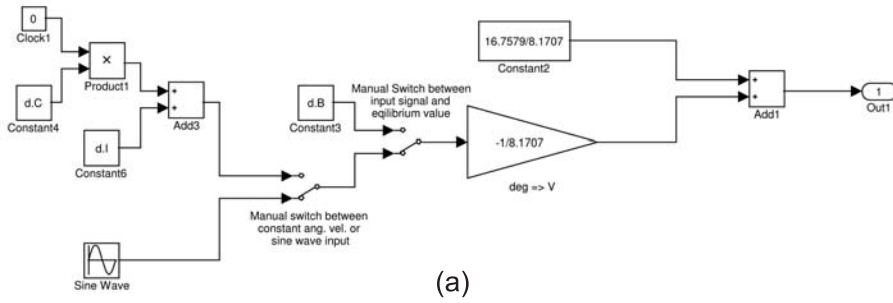


Figure 22: Simulink model of the feedback control



## 6 Measurements with camber sweeps

The aim of this thesis is to develop a feedback control for the actuator on the Flat Plank Tyre Tester. With this feedback control, it is possible to execute measurements on motorcycle tyres with camber sweeps. In this chapter, the results of these measurements are discussed.

### 6.1 Measurements

For the measurements, five specific cases are executed on the Tyre Tester. These cases were already treated in section 5.3 and can be found in table 4. The difference between the measurements in section 5.3 and these measurements is that the plank translates in the latter set of experiments; for cases 1, 3 and 5 is the velocity 0.02 m/s, for cases 2, 4 and 6 is the velocity 0.0475 m/s. Also is the initial vertical load on the tyre set to 1300 N, instead of 1500 N at the former experiments. The maximum translation of the plank is set to 5 meter, to prevent the plank from running out of the pinion that drives the plank. The direction of the plank velocity is defined in figure 23. The road camber angle  $\beta_x$  is negative here because of the clockwise rotation. Note that the wheel camber angle  $\gamma$  is positive in figure 23.

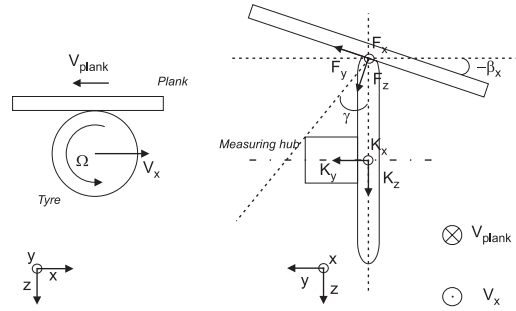


Figure 23: Overview of the tyre and the plank with the interesting forces

In case 3 the angular velocity of the plank is too low to make the measurement useful. In this case, the plank would have turned about  $1.5^\circ$  after 5 meter, or 250 s. Therefore, case 3 is cancelled. Most interesting in the results of the measurements are  $F_y$  and  $F_z$ , like defined in figure 23, which are composed of both  $K_y$  and  $K_z$ , see equations 6 and 7.

$$F_y = K_y \cdot \cos \gamma - K_z \cdot \sin \gamma \quad (6)$$

$$F_z = K_y \cdot \sin \gamma + K_z \cdot \cos \gamma \quad (7)$$

### 6.2 Results and comparison

The results of the measurements described in the preceding chapter are discussed and compared with the results of the experiments described in chapter 2.

#### Pacejka

For case 1 and 2, the relation between  $F_y$  and  $F_z$ , and the angle and the covered distance of the plank are plotted in figure 24.

Remarkable is the non-symmetric shape of both  $F_y$  and  $F_z$ : the equilibrium value of  $F_y$  and  $F_z$  should be 0 N resp. 1300 N, which obviously is not the case. An explanation might be that the tyre does not rotate around the center line of the plank, but it can also have other, unknown causes. It is beyond the scope of this thesis to go more deeply into this behavior.

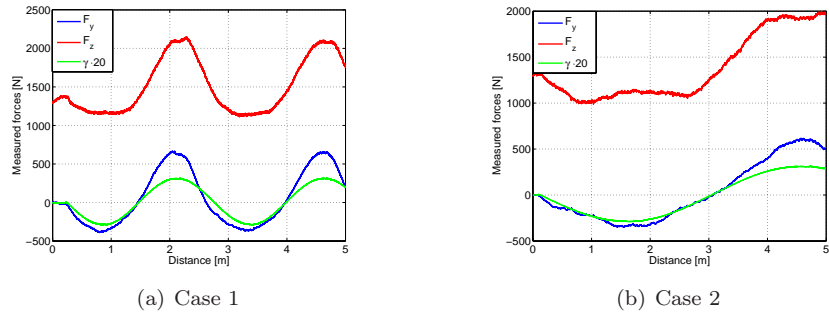


Figure 24:  $F_y$ ,  $F_z$  and the camber angle  $\gamma$  obtained from the measurements plotted against the distance

When these results are compared with the results of the simulations, figure 25, it appears that in both cases the  $F_y$  of the measurements on the Flat Plank is much larger than the  $F_y$  calculated by the mathematical model of Pacejka. This might be due to unknown parameters of the used tyre, which are taken into account in the simulation.

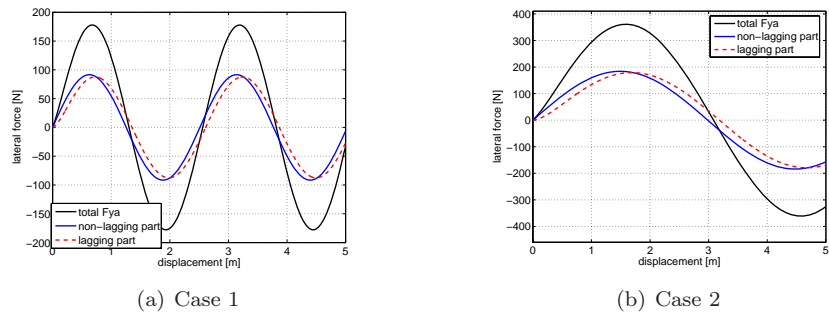


Figure 25: The  $F_y$  obtained from the simulations plotted against the distance

### University of Padova

There is only one measurement available to compare with the results of the experiments done by the University of Padova, namely case 4.

The scope of the measurements of the University of Padova was to investigate the phase lag between the camber motion and the measured force. As noticeable in figure 26, it is hard to distinguish a phase shift because of the noise in the signals. Also it is not possible to derive the expected phase shift from the results of Padova, because their minimum forward velocity is 0.56 m/s, which is ten times the maximum velocity of the Flat Plank. But it is possible to compare it with a mathematical model, used by the University of Padova. From the results of this model, see figure 27, the phase angle between the camber motion and the force should be about  $-14^\circ$ . However, when a sine with the same frequency and amplitude as the camber motion, but with a phase lead of  $14^\circ$ , is plotted, it is clear that the force does not lead the camber motion with an angle of  $14^\circ$ , see figure 26.

### Constant velocity

The results of the measurements with constant angular velocities are plotted in the graphs below. Because the results of the experiments of TNO are unknown, the measurements can not be compared.

The fact that  $F_z$  is obvious not linear, strikes the eye. This behavior can be explained by non-uniformity of the tyre or the fact that the tyre is not mounted on the axis of rotation of the plank, but with a small offset. This is a constructional problem; the tyre can not reach the axis of rotation. At this point it is hard to draw conclusions from these results and make reliable comparisons between these results and results of other measurements, because more variables than just the camber angle or the forward velocity of the plank have influence on the measured forces.

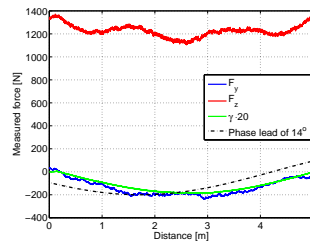


Figure 26:  $F_y$ ,  $F_z$  and the camber angle  $\gamma$  obtained from the measurements plotted against the distance

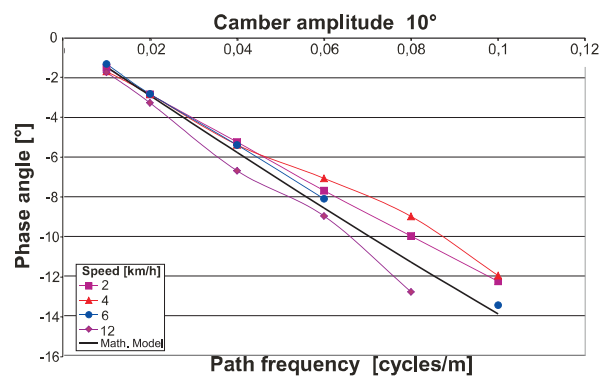


Figure 27: The phase angle plotted against the path frequency for the scooter tyre for a camber amplitude of  $10^\circ$  [3]

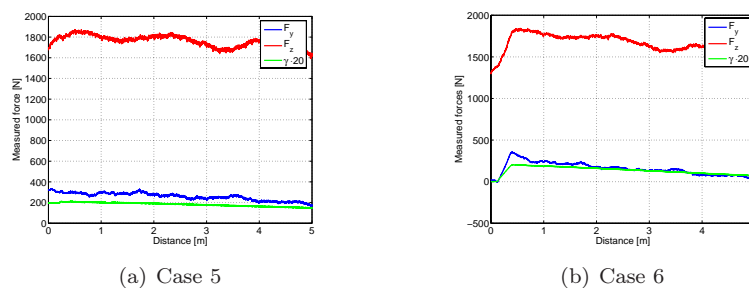


Figure 28:  $F_y$ ,  $F_z$  and the camber angle  $\gamma$  obtained from the measurements plotted against the distance



## 7 Conclusions and recommendations

The aim of this thesis was to design a feedback control for the Flat Plank Tyre Tester. This control makes it possible to execute tests on tyres with camber sweeps. For this purpose, first a mathematical model of tyre dynamics and different experiments with camber sweeps executed by the University of Padova and TNO were considered. Then the current setup of the Tyre tester and its possibilities was investigated and compared with the other experiments. From this, it was concluded that the present actuator on the test stand does not comply to the set demands. Therefore, a new actuator was chosen, based on these shortcomings of the present actuator. This is a linear actuator of the CAP32-series from SKF with a D24CW motor

After the actuator was mounted at the Flat Plank, the frequency response of the actuator was determined and a Bode plot was developed.

For the design of the feedback control, first a proportional gain was tried. A gain of 25 satisfies; the actuator can follow a predefined trajectory with a maximum relative error of 4.34%, dependent on the trajectory.

The feedback control was implemented in a Simulink model and five cases were executed on the Flat Plank with a motorcycle tyre while the plank had a forward velocity. The results of these measurements were compared with the experiments of the other departments. The results did not quite match. It follows that it is hard to draw a conclusion from this, because more variables than the camber sweep and forward velocity of the plank are involved when studying the forces acting on a tyre during cambering.

A reliable comparison between the results of the experiments on the Flat Plank Tyre Tester and the experiments executed by the other authorities can only be made if more variables of the tyre and the different setups are known, because all experiments deal with other motorcycle tyres and test stands. So, more investigation on tyre dynamics is needed for a reliable comparison between the results of the experiments.

Furthermore, executing camber sweep experiments on the Flat Plank will be more easily when the actuator is controlled by the same computer and software as with which the tyre forces are measured. This is possible when the feedback control is implemented in Labview.





## A Effect of the non-lagging part ratio

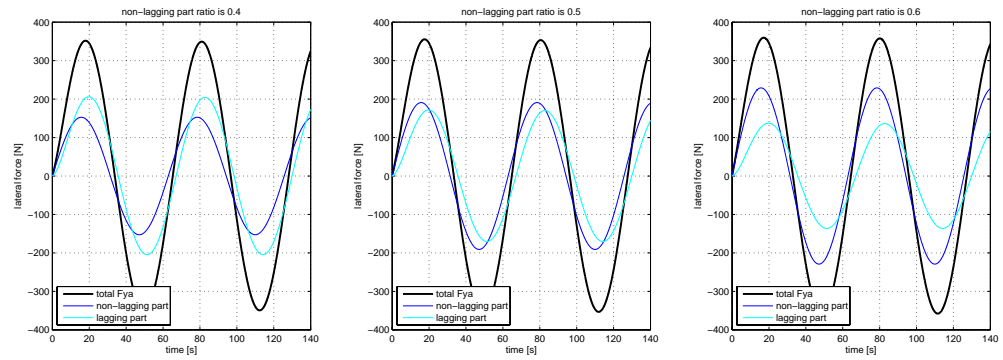


Figure 29: The effect of the non-lagging part ratio  $\varepsilon_{NL}$  on the lagging and non-lagging forces



## B Results of measurements on the flat plank

Table 5: Stroke of the actuator with corresponding angle of actuator, plank and torsion-arm

Stroke (mm)	Angle (degrees)		
	Actuator	Plank	Torsion-arm
0	64.2	14.5	29.3
50	63.2	0	14.6
100	63.8	-14.5	1.1

Table 6: Time it takes the actuator to move in and move out

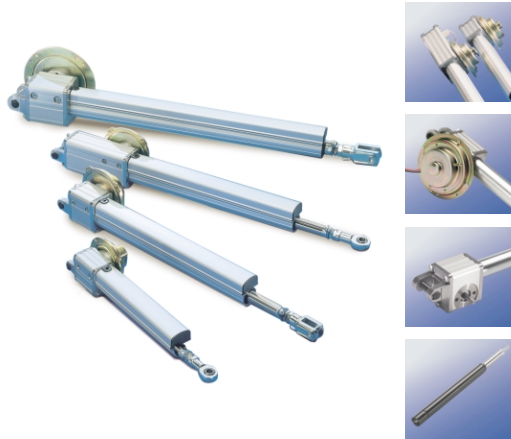
Adj. of potmeter	Time to move in (s)	Time to move out (s)
2	-	-
4	-	-
6	-	-
7	13	10
8	11	8
9	9	7
10	9	7
11	8	6



# C Information about the CAP/CAR32-series



## CAR Linear Actuators



### The CAR Linear Actuators

The CAR range of industrial actuators offers a unique standard of performance, durability and reliability. The compact design incorporates well-proven parts, such as the SKF high efficiency ball screw, a sturdy gearbox assembly and high quality DC and AC-motors. All to give the best possible performance with unsurpassed service life. Individual application requirements can easily be matched thanks to the modular design concept. A vast number of motors, gear ratios and other options can be combined to give the actuator the required characteristics. The CAR range is available in three sizes, CAR22, CAR32 and CAR40, with loads of up to 6000N. Three special versions of the CAR 32 actuator are available:

- CAP 32, with integrated positional feedback potentiometer.
- CARN 32, with gearbox input shaft for external drive source.
- CCBR 32, without motor and gearbox (direct drive on the ball screw).

### Contents

The product range	2
Ordering keys for CAR 22, CAR 32, CAR 40 and CAP 32	3
Performance	4
CAR 22, 32, 40	6
CAP 32	7
CARN 32	8
CCBR 32	9
Motors / Motor data	10
Accessories	12
Options	16
SKF control units	16
Calculations	17

The specifications and data in this publication are believed to be accurate and reliable. However, it is the responsibility of the product user to determine the suitability of all products selected for a specific application. Consult SKF for application support. The right is reserved to make changes without prior notice.

2



### Ordering keys

**CAR 22**

Dynamic load (N) / Speed (mm/sec.)	Motor options	Code
1500/20	1500/20-20	1500/20
1500/30	1500/30-20	1500/30
1500/40	1500/40-20	1500/40

Motor assembly: Right (R), Left (L)

Stroke: 50 mm, 100 mm, 150 mm, 200 mm, 300 mm, 500 mm, 700 mm, 900 mm

Options: Friction clutch (only for CAR32) Back-up nut

**CAR 32**  
**CAP 32**

Dynamic load (N) / Speed (mm/sec.)	Motor options	Code
3500/20	3500/20	3500/20
3500/30	3500/30-20	3500/30
3500/40	3500/40-20	3500/40
3500/50	3500/50-20	3500/50
3500/60	3500/60-20	3500/60
3500/70	3500/70-20	3500/70
3500/80	3500/80-20	3500/80
3500/90	3500/90-20	3500/90
3500/100	3500/100-20	3500/100
3500/110	3500/110-20	3500/110
3500/120	3500/120-20	3500/120
3500/130	3500/130-20	3500/130
3500/140	3500/140-20	3500/140
3500/150	3500/150-20	3500/150
3500/160	3500/160-20	3500/160
3500/170	3500/170-20	3500/170
3500/180	3500/180-20	3500/180
3500/190	3500/190-20	3500/190
3500/200	3500/200-20	3500/200

Motor assembly: Right (R), Left (L)

Stroke: 50 mm, 100 mm, 150 mm, 200 mm, 300 mm, 400 mm, 500 mm, 600 mm, 700 mm, 800 mm, 900 mm, 1000 mm

Options: Friction clutch (only for CAR32) Back-up nut

**CAR 40**

Dynamic load (N) / Speed (mm/sec.)	Motor options	Code
6000/20	6000/20	6000/20
6000/30	6000/30-20	6000/30
6000/40	6000/40-20	6000/40
6000/50	6000/50-20	6000/50
6000/60	6000/60-20	6000/60
6000/70	6000/70-20	6000/70
6000/80	6000/80-20	6000/80
6000/90	6000/90-20	6000/90
6000/100	6000/100-20	6000/100
6000/110	6000/110-20	6000/110
6000/120	6000/120-20	6000/120
6000/130	6000/130-20	6000/130
6000/140	6000/140-20	6000/140
6000/150	6000/150-20	6000/150
6000/160	6000/160-20	6000/160
6000/170	6000/170-20	6000/170
6000/180	6000/180-20	6000/180
6000/190	6000/190-20	6000/190
6000/200	6000/200-20	6000/200

Motor assembly: Right (R), Left (L)

Stroke: 100 mm, 200 mm, 300 mm, 400 mm, 500 mm, 600 mm, 700 mm, 800 mm, 900 mm, 1000 mm

Options: Friction clutch Back-up nut



3

### Performance

DC-motors					AC-motors				
Actuator	Max dynamic load	Max static load	Linear speed	Current consumption	Actuator	Max dynamic load	Max static load	Linear speed	
<b>D24B</b>	N	N	mm/s	A	<b>E220C/E220CB</b>	N	N	mm/s	
CAR 22xSx1	1500	2200	15-10	5	CAR/CAP32xSx1	3500	2500	1500	5400
CAR 22xSx2	1000	2200	30-20	5	CAR/CAP32xSx2	2500	1500	900	5400
CAR/CAP 32xSx4	1500	5400	60-40	8	CAR/CAP 32xSx4	1500	900	500	5400
<b>D24C/D24CS/D24CB</b>					<b>E110C/E110CB</b>				
CAR/CAP 32xSx1	3500	5400	15-10	8		25µF	16µF	12µF	
CAR/CAP 32xSx2	2500	5400	30-20	8	CAR/CAP 32xSx1	3500	2500	1500	5400
CAR/CAP 32xSx4	1500	5400	60-40	8	CAR/CAP 32xSx2	2500	1500	900	5400
<b>D24CW</b>					CAR/CAP 32xSx4	1500	900	500	5400
CAR 32xSx1	3500	5400	9-5	5	<b>E220D/E220DB</b>				
CAR 32xSx2	2500	5400	18-10	5		12µF	8µF		
CAR 32xSx4	1500	5400	34-24	5	CAR 40xSx1	6000	4000	8700	9
<b>D24D/D24DS/D24DB</b>					CAR 40xSx2	4000	2700	8700	17
CAR 40xSx1	6000	8700	15-10	16	CAR 40xSx4	2000	1200	8700	34
CAR 40xSx2	4000	8700	30-20	16	<b>E110D/E110DB</b>				
CAR 40xSx4	2000	8700	60-40	16		37.5µF	25µF		
<b>D12B</b>					CAR 40xSx1	6000	4000	8700	10
CAR 22xSx1	1500	2200	15-10	9	CAR 40xSx2	4000	2700	8700	20
CAR 22xSx2	1000	2200	30-20	9	CAR 40xSx4	2000	1200	8700	40
<b>D12C</b>									
CAR/CAP 32xSx1	2500	5400	15-10	13					
CAR/CAP 32xSx2	2000	5400	30-20	13					
CAR/CAP 32xSx4	1000	5400	60-40	13					

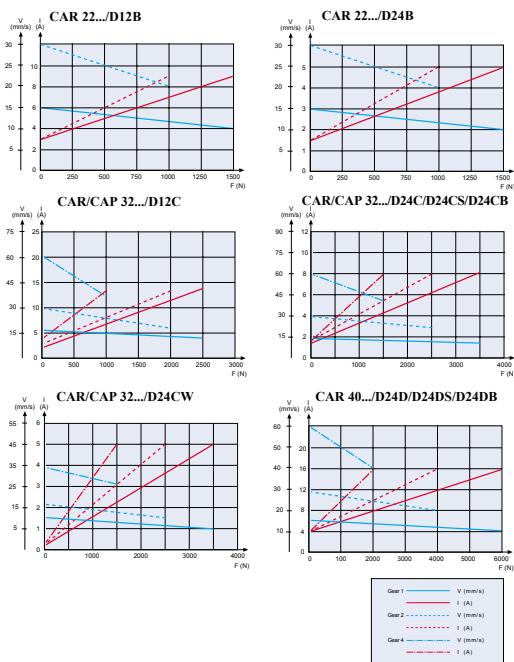
The CAR actuator range is self-locking within the dynamic load range with gear (1). Gear (2) and (4) are self-locking within the dynamic load range if a DC-motor with brake is used.

CAR actuators equipped with AC-motors are self-locking within the dynamic load range if a brake is used.

4



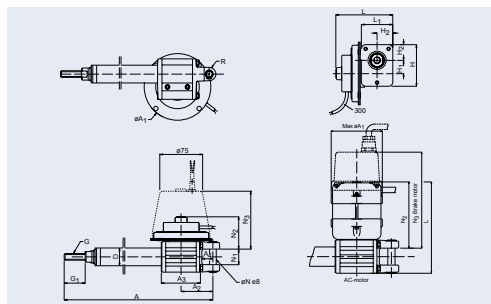
Performance diagram



SKF

5

CAR 22, 32, 40



Actuator	A	A2	A3	A4	D	G	G1	H	H1	H2	L1	N	N1	R
CAR 22	S-205	49	66	16	22	M10 x1.5	35	60	16.5	23	46	10	26	9
CAR 32	S-218	57	71	20	32	M12 x1.75	38	73	23	27.5	55	12	28	12
CAR 40	S-263	75	100	25	40	M16 x2	53	97	29	40	80	16	40	19

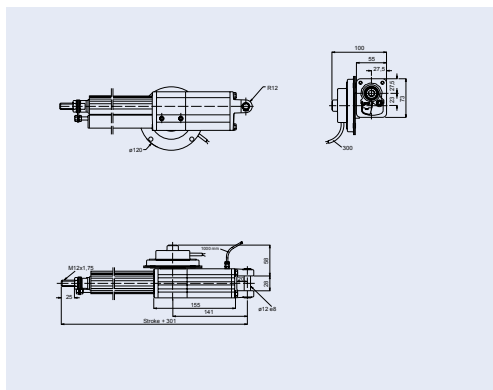
Motor	A1	L	N2	N3	Stroke S		Weight
					mm	kg	
D12B	104	86	53	-	CAR22	50	1.2
D12C	120	100	58	-		100	1.3
D24B	104	86	53	-		150	1.4
D24C	120	100	58	-		200	1.5
D24CW	120	100	58	-		300	1.6
D24CS	120	100	58	-	CAR32	50	2.1
D24CB	120	141.5	58	100		100	2.2
D24D	150	127	75	-		200	2.4
D24DS	150	127	87	-		300	2.7
D24DB	150	181	75	121		500	3.2
E110C	97	150	108	-		700	3.7
E110CB	97	198	-	156	CAR40	100	5.8
E110D	119	200	141	-		300	6.7
E110DB	119	248	-	189		500	7.6
E220C	97	150	108	-		700	8.4
E220CB	97	198	-	156			
E220D	119	200	141	-			
E220DB	119	248	-	189			

The CAR actuator is manufactured in three versions with capacities up to 6000 N. The CAR 32 and 40 versions can be supplied with three gear ratios (1, 2, 4) while the CAR 22 is available with two ratios (1, 2). With gear 1, the CAR actuator is self-locking within the dynamic load range, when used together with DC-motors. Actuators fitted with gear 2 & 4 are self-locking within the dynamic load range provided that a motor with brake is fitted. CAR actuators equipped with AC-motors are self-locking within the dynamic load range providing motors with brakes are fitted. The friction clutch protects the actuator and the mechanism to which it is fitted from damage caused by dynamic overload.

6

SKF

CAP 32



The CAP 32 actuator is fitted with a potentiometer which indicates the position of the actuator. This unit is, therefore, suitable for use in situations where it is necessary to know the current position of the actuator, either for manual or automatic control. The CAP 32 has a built in 10kΩ potentiometer which is

Positioning accuracy	Accuracy
mm	
1	±1
2	±2
4	±4

At constant load and direction of load a significantly higher accuracy can be achieved. Please consult SKF for further information.

linked to the ball screw. This provides an analogue signal representing the present position of the adjustment tube. The CAP 32 is fitted, as standard, with CAXB limit switch. Other performance values are identical with CAR 32.

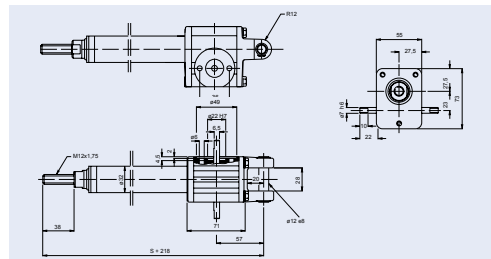
Stroke S	Weight	
	mm	kg
CAP32	50	2.9
	100	3.3
	200	3.7
	300	4.1
	500	4.5
	700	5.0

Ordering key - see page 3.

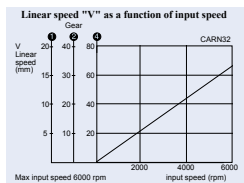
SKF

7

CARN 32 actuator without motor



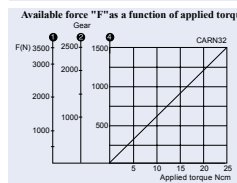
An external drive can be connected to CARN 32. This could be a pneumatic motor, a manual drive unit or an electric motor, linked to the gearbox input shaft. The CARN 32 actuator can also be operated in parallel with two, or more, actuators. The linear speed is determined by the input rotary speed, as shown in the diagram below. A diagram also shows the torque required for any given load.



8

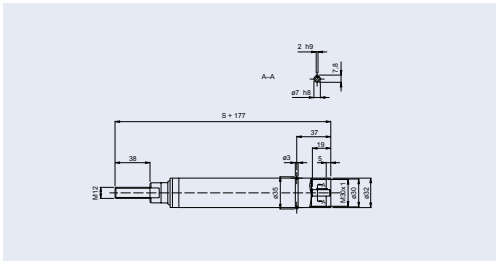
Stroke S	Weight	
	mm	kg
CARN32	50	0.8
	100	1.0
	200	1.5
	300	2.2
	500	2.7
	700	3.3

Designation	Gear ratio	Ballcrew lead
CARN 32xSx1	25.0:1	4
CARN 32xSx2	12.5:1	4
CARN 32xSx4	6.25:1	4



SKF

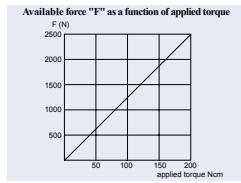
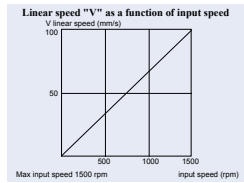
### CCBR 32 actuator without motor



The CCBR 32 is an actuator with no motor or gearbox. It is driven directly by the ball screw and is therefore of small external dimensions. Direct drive offers very accurate positioning. The SKF ball screw provides a high level of efficiency. The linear speed is determined by the input rotary speed, as shown in the diagram below. A diagram also shows the torque required for any given load. If required, the CAXB 32 limit switch can be mounted on the ball screw cylinder. The front mounting attachment described in page 12 is also suitable for CCBR 32. A steel ring to be mounted at the end of the cylinder is supplied with CCBR 32. The drawing shows the ring fitted to the cylinder.

Stroke S	Weight	
	mm	kg
CCBR32	50	1.1
	100	1.2
	200	1.25
	300	1.3
	500	1.4
	700	1.5

Designation	Max dyn. load	Max stat. load	Ball screw lead
Ordering key	N	N	mm
CCBR 32xS	2500	5400	4



### Motors

SKF actuators are fitted with either AC or DC-motors.

#### DC-motors

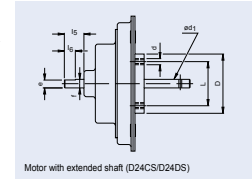
12 and 24 Volt motors are available. CAR and CAP 32 are fitted with compact flat motors. DC-motors are simple to control but have a limited service life, due to the wear of the brushes and commutator. The 'General motor data' table on page 11 shows the approximate service life when operated at rated power. The flat motors are protected against dust and moisture, to protection class IP44. The connecting cables on all flat motors are 300 mm in length.

#### AC-motors

120 and 230 Volt motors are available. The 230V motors are fitted with thermal protection. AC-motors are protected against dust and moisture, to protection class IP54 (with brake IP20). The motors for CAR 32 and 40 are fitted with connecting cables 1000 mm in length. A start capacitor is required for the operation of AC-motors. For selection of capacitor see page 18 (calculation section).

#### Motors with extended shaft

These motors are suitable for situations where it is necessary to synchronize the actuators. The shaft can then be linked to the extended shaft or another motor or to the shaft of a CARM 32 actuator. The extended shaft can also be used to adjust the actuator manually with a hand wheel, for example, in case of power failure. Motors with extended shaft are available in the 24 V DC range for use on the CAR 32, 40 and CAP 32.



Actuator size	Motor type	Dimensions D	Dimensions						
			d	d1	e	f	I5	I6	L
CAR 32	D24CS	48mm	M5	7hg	6.5	7h7	16	9	36
CAR 40	D24DS	70mm	M8	9hg	6.5	7h7	16	9	55

### General motor data

Designation	Rated voltage	Rated speed	Brush life
<b>DC-motors</b>			
	V DC	rpm	hours
D12B	12	7600	300
D12C	12	5300	1500
D24B	24	7500	500
D24C	24	5500	1500
D24CB	24	5500	1500
D24CW	24	2500	1500
D24CS	24	5500	1500
D24D	24	4700	900
D24DB	24	4700	900
D24DS	24	4700	900
<b>AC-motors</b>			
	V AC	rpm	
E220C	230/50Hz	2600	-
E220CB	230/50Hz	2600	-
E220D	230/50Hz	2790	-
E220DB	230/50Hz	2790	-
E110C	120/60Hz	3250	-
E110CB	120/60Hz	3250	-
E110D	120/60Hz	3350	-
E110DB	120/60Hz	3350	-

### Accessories

#### Mounting attachments

SKF mounting attachments provide simple and secure mounting of the actuators. There are various types for attachment both to front and rear of the actuator. The mounting attachments are supplied complete with nuts and bolts.

#### Front mounting attachments

##### Rod-end, Type 575

The rod-end allows some alignment of the actuator. The rod-end requires no maintenance and consists of a head with an inner pivot bearing and a bearing surface located between the hole in the head and the inner ring. The rod-end is made of galvanized steel. The unit is supplied complete with lock nut. Mounting attachment Type 575 must not be combined with Type 581.

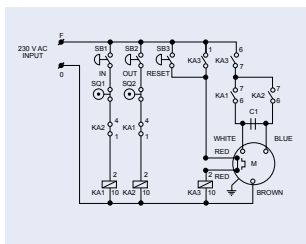
Rod-end Designation	Appropriate for linear actuator No.	Dimensions							Degrees of freedom
		A	B	d	G	G1	H	H1	
575-22	22	30	14	10	M10	15	43	5	13
575-32	32	34	16	12	M12	18	50	6	13
575-40	40	42	21	16	M16	24	64	8	15

##### Clevis attachment, Type 576

This consists of a galvanized clevis head and a journal fitted with a quick coupling. It allows simple and rapid attachment of the actuator. This mounting attachment is supplied complete with locking nut.

Clevis Designation	Appropriate for linear actuator No.	Dimensions						
		d	G	H	H1	H2	H3	N
576-22	22	10h11	M10	40	20	12	5	20
576-32	32	12h11	M12	48	24	14	6	24
576-40	40	16h11	M16	64	32	19	8	32

### Recommended wiring diagram for general connection of CAR with 230/120 V AC-motors



A low voltage limit switch (CAXB) can be used in connection with SKF special electronic control systems. As standard, motors are fitted with thermo-contacts which activates at +140°C.

SB = operating switch  
SQ = limit switch  
KA = relay  
C1 = capacitor  
M = motor



## Accessories

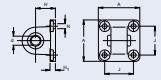
### Mounting attachments

#### Rear mounting attachments

##### Rear mounting bracket, Type 580

The bracket consists of an eye on a base plate, made of light alloy, with a bronze bush vulcanized into the ring of the eye. This gives some degree of flexibility to the attachment and the rubber also has a vibration damping effect. The unit is supplied complete with attachment bolts.

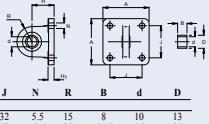
Bracket Designation	Appropriate for linear actuator No.	Dimensions						
		A	d	H	H1	J	N	R
580-22	22	46	10	22	6	32	5.5	
580-32	32	55	12	28	12	40	6.6	
580-40	40	80	16	36	15	59	9	



##### Ball-joint bracket, Type 581

This bracket is intended for mounting at the rear of the actuator. It consists of an eye on a base plate, made of light alloy, with a pivoted bearing in the eye ring. This allows some degree of self-alignment. This bracket should not be used if the actuator is fitted with a friction clutch. The bracket is supplied complete with two spacer rings and attachment bolts. Mounting attachment Type 581 must not be combined with Type 575.

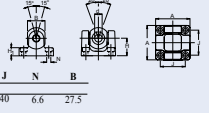
Bracket Designation	Appropriate for linear actuator No.	Dimensions										
		A	d	H	H1	J	N	R	B	d	D	
581-22	22	46	10	22	6	32	5.5	15	8	10	13	
581-40	40	80	16	36	11	59	9	25	11.5	16	20	



##### Universal bracket, Type 582

This bracket is moulded in aluminum, and consists of a plate with an integrated ball, which has an attachment hole. The ball is guided, so it can be misaligned ( $\pm 15^\circ$ ) horizontally and ( $\pm 20^\circ$ ) vertically. This feature will allow some degree of misalignment, and make it possible to mount the actuator on an uneven surface.

Bracket Designation	Appropriate for linear actuator No.	Dimensions					
		A	d	H	H1	J	N
582-32	32	55	12	28	13	40	6.6



SKF

13

## Accessories

### Limit switch CAXB

Limit switches, in combination with an SKF control unit make it possible to set the actuator for any desired stroke length. They also protect the actuator from running against the mechanical end stops, thereby avoiding damage.

The CAXB limit switch can be used on the following ball screw actuator: CAR, CAP, CARN and CCBR. It is robust and durable and can be used in most environments. CAXB limit switches are available in a number of standard lengths, but can be manufactured in special lengths on request.

The CAXB limit switch consists of a profiled tube, two switch units, a rod carrying a permanent magnet and a protective cover.

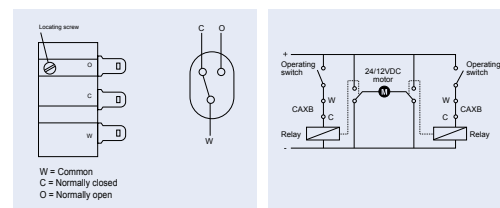
The profiled tube, which is made of anodized aluminum, is mounted directly on the protection tube of the actuator.

The two switch units (proximity switches) are attached to the profiled tube and can be adjusted to any position. The magnet rod, made of stainless steel, is attached to the end of the adjustment tube and runs in a groove in the profiled tube.

When the magnet, which is attached to the free end of the rod, approaches the switch unit, the latter is activated. The switches are connected to the control unit, from which relays disconnect the power supply to the motor. The motor is then short-circuited, thereby braking the actuator.

The switches and connections are effectively protected by an anodized aluminum cover. There are three connections to the switch units, allowing them to be connected in "normally open", "normally closed" or "alternating" modes (see illustration below).

In order to minimize the stopping distance of the actuator and to ensure correct circuit-breaking, the actuator should be connected as shown in the wiring diagram below.



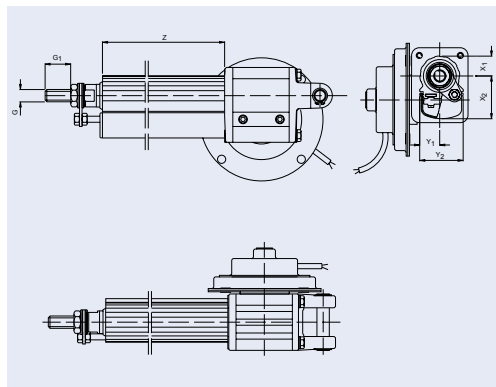
Permissible brake power 3 W  
Max brake voltage 200 V DC  
Max brake current 200 mA DC  
The switches must not be connected to an AC supply.

14

SKF

## Accessories

### Limit switch CAXB



Designation	Dimensions			Y2	Z	G	G1
	X1	X2	Y1				
CAXB 22x50	14	37	22	42.5	120	M10x1.5	25
CAXB 22x100				170			
CAXB 22x150				220			
CAXB 22x200				270			
CAXB 22x300				370			
CAXB 32x50	20	42	20	42.5	120	M12x1.75	25
CAXB 32x100				170			
CAXB 32x200				270			
CAXB 32x300				370			
CAXB 32x500				570			
CAXB 32x700	770						
CAXB 40x100	23	46	19	42.5	170	M16x2	35
CAXB 40x300				370			
CAXB 40x500				570			
CAXB 40x700				770			

SKF

15

## Options

#### Friction clutch

All CAR actuators, except size 22, can be equipped with a friction clutch. The friction clutch is not intended for use as a load limiter, but only for protection of the actuator and the mechanism to which the actuator is fitted, in the event of dynamic overload.

#### Back-up nut

CAR 32 and CAR 40 can be fitted with a back-up nut in cases where added safety is required. The ball nut is then equipped with a device which prevents the ball nut moving axially, in case of failure.

## SKF Control units

	CAEL 10-24R	CAEN 10R	CAEP 10P-SL	CAED 5-24R	CAED 9-24R	CAEV 110-220
<b>DC Motor</b>						
D24B				X		
D24C	X	X	X		X	
D24CS	X	X	X		X	
D24CB	X	X	X		X	
D24CW				X		
<b>AC Motor</b>						
E110C						X
E110CB						X
E220C						X
E220CB						X
<b>Limit switch</b>						
CAXB	X	X	X	X	X	X
<b>Hand switch</b>						
CAES 31B	X	X	X	X	X	X
CAES 31C						

16

SKF

**Calculations**  
**Life calculation**

The service life of a CAR actuator is normally determined by the  $L_{10}$  life of the ball screw. In most cases there is less wear on the worm gear and bearings than on the ball screw. Under certain circumstances the life of the motor is shorter than that of the ball screw, however, the motor can be easily replaced. The table, page 11, shows the life of various DC-motors at rated output power. Generally, the life of DC-motors is reduced when load and number of starts/stops is increased. To calculate the basic rating life  $L_{10}$  of ball screw it is sufficient if the dynamic load and actual stroke is known.  $L_{10}$  is defined as the life that 90% of a sufficiently large group of apparently identical ball screws can be expected to attain or exceed.

$$L_{10} = \frac{500 \cdot 000 \cdot x_D}{S} \times \left(\frac{C}{F_w}\right)^3$$

$L_{10}$  = basic rating life in double strokes i.e. a stroke from one end position to the other and back again.  
 $p$  = lead of the ball screw mm (CAR 22, 2.5 mm, CAR 32, 4 mm, CAR 40, 5 mm).  
 $S$  = actual stroke (mm).  
 $C$  = ball screw basic dynamic load rating (N)  
 CAR 22, 1500N, CAR 32, 3500N, CAR 40, 6000N.  
 $F_w$  = cubic mean load (N).  
 In many cases, the magnitude of the load fluctuates. In order to calculate the equivalent screw load, it is first necessary to determine a constant mean load  $F_w$  which would have the same influence on the ball screw as the actual fluctuating load. A constant mean load can be obtained from the formula below.

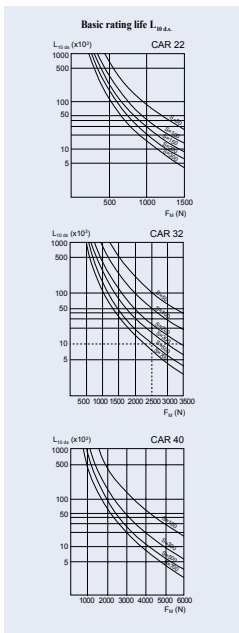
$$F_w = \sqrt[3]{\frac{F_1^3 \times S_1 + F_2^3 \times S_2 + F_3^3 \times S_3 + \dots}{S_1 + S_2 + S_3 + \dots}}$$

$F_1, F_2, F_3, \dots$  = cubic load (N) during  $S_1, S_2$  and  $S_3$  partial stroke.  
 The diagrams show life in double strokes,  $L_{10}$ , at various load and stroke.

**Example:**  
 CAR 32x500x1D24C having a load of 2800N in one direction of movement and 2100N in the other. The entire stroke of the actuator is utilized.

$$F_w = \sqrt[3]{\frac{2800^3 \times 500 + 210^3 \times 500}{500 + 500}} = 2500 \text{ N}$$

Diagram for CAR 32 shows  $L_{10} = 10000$  double strokes

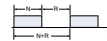


**Calculations**  
**Duty factor**

SKF Linear Actuators are designed for intermittent operation. Permitted load is related to the duty factor i.e. load must be reduced when the duty factor is increased. In the diagrams maximum load is shown as a function of duty cycle. A capacitor must be selected for AC-actuators. The diagrams show required capacitor size at various load and duty factor. If the recommended duty factor is exceeded the actuator may be overheated and damaged. Duty factor is defined as amount of time running under load versus total cycle time.

$$\text{Duty factor \%} = \frac{N}{N+R} \times 100$$

$N$  = running under load  
 $R$  = rest period  
 $N+R$  = total cycle time



Permitted load for DC-actuators at a specific duty factor is expressed in percentage of maximum dynamic load capacity (see diagram).

**Example:**  
 A CAR 40x700x2D24D is running with the following cycle: 5 seconds running, 5 seconds rest, 5 seconds running, 15 seconds rest, and so on.

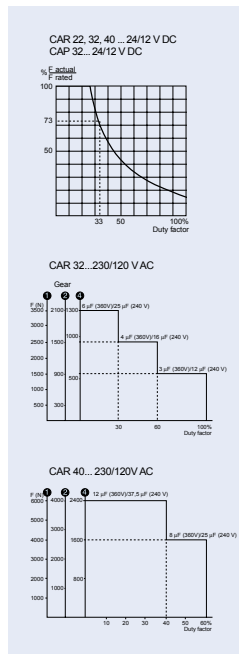
Calculate duty factor and maximum load for this working cycle.

$$\text{Duty factor} = \frac{5 + 5}{(5 + 5) + (5 + 15)} \times 100 = 33 \%$$

Diagram shows that permitted load ( $F_{p, \text{duty}}$ ) is 73% of maximum dynamic load at 33% duty factor.

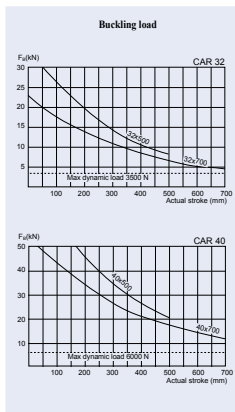
Max dynamic load = 5000 N  
 Permitted load = 0.73x5000=3650 N.

**Note:**  
 All diagrams are valid for a maximum ambient temperature of +20°C. At higher temperatures or in critical applications, please contact SKF.



**Calculations**  
**Buckling safety factor**

At max. dynamic load the buckling safety factor exceeds 2 for all actuators with standard stroke, except CAR 32 with a stroke of 700 mm. The diagrams below, show the buckling load for CAR 32 and 40 with 500 and 700 mm strokes. As shown, the buckling load varies with the actual stroke. If the required stroke exceeds the maximum standard stroke, please contact SKF.



**Selection**  
**Wire dimension for DC-Motors**

Long lead wires between the power source and the actuator will result in a voltage drop for DC-units. The wires should be selected so that the voltage drop does not exceed 5% of rated voltage. Required wire dimension can be calculated using the following formula:

$$a = 0.4 \times L \times \frac{I}{U}$$

$a$  = cross section area of the wire (mm<sup>2</sup>)  
 $L$  = total wire length in the both directions (m)  
 $I$  = current consumption (A)  
 $U$  = supply voltage (V DC)

**Example:**  
 $L = 5 \text{ m}$   
 $I = 14 \text{ A}$   
 $U = 12 \text{ V DC}$

$$a = 0.4 \times 5 \times \frac{14}{12} = 2.3 \text{ mm}^2$$

i.e. select nearest standard wire:  $a=2.5 \text{ mm}^2$

**Temperatures**  
 The CAR actuator can normally be used within a temperature range -20°C to +70°C. All performance data stated in the catalogue are only valid at +20°C.



**SKF Actuation Systems - Product groups**



**Contacts**

- Austria**  
**Linear Motion**  
**SKF Österreich AG**  
 Phone +43 2236 6709 0  
 Fax +43 2236 6709 220  
 E-mail multitec.austria@skf.com
- Belgium**  
**SKF Multitec Benelux B.V.**  
 Phone +31 650 4629 028  
 Fax +31 650 4629 028  
 E-mail multitec.belux@skf.com
- Denmark**  
**SKF Multitec**  
 Phone +45 65 92 77 77  
 Fax +45 65 92 74 77  
 E-mail multitec.denmark@skf.com
- Finland**  
**SKF Multitec**  
 Phone +358 20 7400 754  
 Fax +358 20 7400 796  
 E-mail multitec.finland@skf.com
- France**  
**SKF Equipements**  
 Phone +33 1 30 12 73 00  
 Fax +33 1 30 12 69 69  
 E-mail equipements.france@skf.com
- Germany**  
**Magnetic Elektromotoren GmbH**  
 Phone +49 7622 695 0  
 Fax +49 7622 695 100  
 E-mail magnetic.germany@skf.com  
**SKF Linearssysteme GmbH**  
 Phone +49 9721 657 0  
 Fax +49 9721 657 111  
 E-mail lin.sales@skf.com
- Italy**  
**SKF Multitec S.p.A.**  
 Phone +39 011 22 49 01  
 Fax +39 011 22 49 213  
 E-mail multitec.italy@skf.com
- Norway**  
**SKF Multitec**  
 Phone +47 22 90 50 00  
 Fax +47 22 30 28 14  
 E-mail multitec.norway@skf.com
- Spain & Portugal**  
**SKF Productos Industriales S.A.**  
 Phone +34 93 377 90 77  
 Fax +34 93 374 2039 / 3156 1256  
 E-mail prod.ind@skf.com
- Sweden**  
**SKF Multitec**  
 Phone +46 42 235000  
 Fax +46 42 235485  
 E-mail multitec.sweden@skf.com
- Switzerland**  
**Magnetic**  
 Phone +41 52 365 02 02  
 Fax +41 52 365 02 06  
 E-mail magnetic.switzerland@skf.com  
**Linear Motion**  
 Phone +41 825 81 81  
 Fax +41 825 82 82  
 E-mail skf.linemove@skf.com
- USA**  
**Magnetic Corporation**  
 Phone +1 618 952 36 47  
 Toll free +1 800 815 6234  
 Fax +1 618 952 00 33  
 E-mail magnetic.usa@skf.com  
**SKF Motion Technologies**  
 Phone +1 610 961 6000  
 Toll free +1 800 541 3024  
 Fax +1 610 961 4811  
 E-mail motiontech.usa@skf.com
- All other countries**  
**SKF Equipements, Strategic Markets**  
 Phone +33 1 30 12 68 52  
 Fax +33 1 30 12 68 59  
 E-mail strategicmarkets.linemove@skf.com

Represented by:





## D Dynamic model

This section describes the dynamic model of the Flat Plank. However, because a lot of influences and their role in the setup are unknown and estimated, the model is rather unreliable. In addition, the dynamics of the devices between the laptop and the actuator is unknown. A lot of time might be spend by fine-tuning the control, perhaps by trial and error. Therefore, it is not used.

The second law of Newton for rotation is used for the dynamic model

$$M = J \cdot \ddot{\delta} \quad (8)$$

In which  $J$  is the mass moment of inertia [ $kg \cdot m^2$ ] and  $M$  is the moment [ $N \cdot m$ ], which equals

$$M = \sum_{i=1}^n F_i \cdot r_i \quad (9)$$

Only two forces are important in this dynamic model, namely the force of the actuator and the friction forces in the bearings. Because it concerns a rotational motion the force exerted on the plank by the tyre can be neglected, since this force goes through the axis of rotation. Also the rolling of the tyre under the plank during a camber sweep can be neglected for this reason.

### Mass moment of inertia

The moment of inertia of a beam around its longitudinal axis is given by

$$J = \frac{m \cdot (h^2 + w^2)}{12} \quad (10)$$

With a density of  $7800 \text{ kg/m}^3$  and a volume of the plank of  $0.0375 \text{ m}^3$ , the mass of the plank is  $292.5 \text{ kg}$ . The height of the plank is  $0.02 \text{ m}$  and the width  $0.25 \text{ m}$ . So, the mass moment of inertia of the plank is  $1.533 \text{ kg} \cdot \text{m}^2$ . Also the mass moment of inertia of the upper shaft can not be neglected. The mass moment of inertia of a shaft around its longitudinal axis is given by

$$J = \frac{m \cdot r^2}{2} \quad (11)$$

With a radius of  $0.025 \text{ m}$ , a length of  $7.54 \text{ m}$  and a density of  $7800 \text{ kg/m}^3$ , the mass of the shaft is  $115.5 \text{ kg}$  and the mass moment of inertia of the shaft is  $0.0361 \text{ kg} \cdot \text{m}^2$ . The total mass moment of inertia of the plank is  $1.569 \text{ kg} \cdot \text{m}^2$ .

### Friction forces

The plank is supported by three types of bearings: four bearings to support the upper shaft, 19 bearings for the rotation of the plank around the lower shaft and 40 in the points of rotation of the rods between the upper and the lower shaft; all are plain bearings. The friction torque in a plain bearing is

$$M_{bearing} = F \cdot f_c \cdot r_s \quad (12)$$

With:  $F$  the radial force on the bearing  $f_c$  the coefficient of friction for rolling bearings and  $r_s$  the radius of the shaft. The 40 bearings in the rods have no lubrication; the bearings contain bronze, in which the steel glides. This involves a coefficient of friction of about 0.3. The other 23 bearings are dry too, but contain a synthetic called Glycodur<sup>®</sup>, which has a coefficient of friction of 0.1. The radial forces on de bearings of the rods and the upper shaft is the force due to gravity minus the force exerted on the Plank by the tyre. Putting this all together, the total friction force due to bearings will be about  $(F_{act}-2870) \cdot 0.18 \text{ Nm}$ .

### Force exerted by the actuator

The moment exerted on the plank by the actuator changes during the motion, because the angle under which the actuator exerts the force via the torsion arm on the plank changes when the angle of the plank changes. This means that the distance  $r$  between the point of rotation of the upper axis and the point of action of the force of the actuator changes. The relation between this distance  $r$  and the angle of the plank is a complex non-linear function. However, the difference between the largest angle and the smallest angle is about 1 degree. This means a difference in the moment of 0.86%, or e.g. 3 Nm when an exerted force of 2000 N is taken. It can be advisable in this situation to neglect this change and assuming that the change of the moment given by the actuator does not have a large influence on the outcome. When it turns out in the end that this assumption is erroneous, the case can be reconsidered.

If  $r$  will be threaten as a constant, its value is

$$r = 0.175 \cdot \cos(1.10) \quad (13)$$

in which 0.175 the length of the torsion-arm and 1.10 the average angle between the torsion-arm and the actuator, in radians. So,  $r=0.0794$  m.

With the above mentioned calculations and assumptions, the dynamic model of the Flat Plank is

$$1.569 \cdot \ddot{\delta} = (F_{act} - 2870) \cdot 0.18 + 0.0794 \cdot F_{act} \quad (14)$$

with  $\ddot{\delta}$  the angular acceleration of the plank and  $F_{act}$  the force exerted by the actuator on the plank. The exerted force of the actuator is dependent on the input voltage and current of the DC-motor and the gear between the DC-motor and the linear part of the actuator itself. In the end, it is decided not to work out this dynamic model and make it useful for the development of the feedback control, because of all unknown and uncertain parameters.

## E Manual of the intermediate device

The intermediate device, already mentioned in chapter five, is the central unit of the connection between the actuator and the laptop. The main part of it is the Maxon current regulator. This device regulates the outgoing current by the incoming voltage, to be brief. The manual of the regulator is included at the end of this section .

### E.1 The connection of the actuator

For the correct operation of the actuator it is important that all five devices -with the intermediate device being the central unit- are connected properly. Before starting, make sure that all devices are turned off or disconnected from the electricity grid to prevent sudden, unexpected movements of the actuator. The intermediate device has a port for the actuator (right) and two for the power supply (left) at its back in figure 30(a). At the front it has a port for the feedback signal of the position labeled "pos" (right in figure 30(b)). This is used for the safety switch. Furthermore, there is a port for the signal coming from the TUE DACS and three ports for the feedback signals of the position of the actuator, the current and the number of revolutions of the DC-motor.



(a) Front of the TUE DACS, the intermediate device and the power supply



(b) Back of the TUE DACS, the intermediate device and the power supply

Figure 30: The connections between the TUE DACS, the intermediate device and the power supply

The connection of the actuator is rather simple, since all ports, except one, are occupied by plugs. First, connect the actuator at the back of the intermediate device by the large grey plug and at the front by the smaller black plug. Then connect the TUE DACS by a cable between output port "DAC1" of the TUE DACS and input port "C ex" at the front of the intermediate device for the input voltage of the current regulator. Furthermore, attach a cable between the output port "pos" at the front of the device and input port "ADC1" of the TUE DACS for the position signal and a cable between "A" or "I" and "ADC2" for the current resp. the number of revolutions of the DC-motor. When working with Labview on the PC, also the "pos"-port must be connected with the device used for the signals from the measurement hub of the tyre by means of a cable and a T-part on the "pos"-port. Since the TUE DACS has only two output ports, a choice between the output ports "A" and "I" must be made, on the assumption that port "pos" will be used always. Now, the power supply can be connected by two wires at the back of the intermediate device.

### E.2 Driving the actuator

The actuator can be driven from a laptop, by the TUE DACS or manually by the intermediate device. Hereto, a switch is applied at the front of the device: the laptop drives the actuator when the switch is turned to the left and when it is turned to the right, it is driven manually. The velocity of the actuator can in the last situation be regulated by a control, called "C man". The counter on the control counts

from 0 to 9. When the counter is set to 5, the actuator does not move. For a value between 0 and 5 the actuator moves inward, with a high speed for a value 0 and a very low speed for a value of almost 5. For a value between 5 and 9 the actuator moves outward, with a high speed for a value 9 and a very low speed for a value of almost 5. Always check the counter before the switch is turned over to the manual control of the actuator.

### **E.3 Safety switch**

An important feature of the intermediate device is the safety switch, which prevents the actuator from moving in or out too far. If this happens, the actuator might fail. When the actuator moves too far, the override stops the actuator. However, the actuator can not be moved back by just turning the manual control in the right direction. First, the switch called "override" must be pushed down to turn off the safety switch. After a few millimeters, the switch can be let go and the actuator moves further. It is important that when the override is switched, the manual control is set to the opposite direction. Otherwise, the safety switch does not work, because of the override, which might lead to failure of the actuator.

# E.4 Manual Maxon current regulator

**maxon motor**

**maxon motor control    4-Q-DC Servoamplifier ADS 50/5**

**Order number 145391**

**Operating Instructions    April 2006 Edition**

The ADS 50/5 is a powerful servoamplifier for driving permanent magnet DC motors up to 250 Watts.

Four modes can be selected by DIP switches on the board:

- Speed control using tacho signals
- Speed control using encoder signals
- IxR compensated speed control
- Torque or current control

The ADS 50/5 is protected against excess current, excess temperature and short circuit on the motor winding. With the FET power transistors incorporated in the servoamplifier, an efficiency of up to 95 % is achieved. A built in motor choke combined with the high PWM frequency of 50 kHz allows the connection of motors with a very low inductivity. In most cases an external choke can be omitted.

Thanks to the wide input power supply range of 12 - 50 VDC, the ADS 50/5 is very versatile and can be used with various power supplies. The aluminium housing makes installation simple, with terminal markings for easy connection.



### Table of Contents

1 Safety Instructions .....	2
2 Performance Data .....	3
3 Minimum External Wiring for Different Modes of Operation .....	4
4 Operating Instructions .....	5
5 Functions .....	7
6 Additional Possible Adjustments .....	10
7 Operating Status Display .....	12
8 Error Handling .....	13
9 EMC-compliant installation .....	13
10 Block Diagram .....	14
11 Dimension Drawing .....	14

The latest edition of these operating instructions may be downloaded from the internet as a PDF-file under [www.maxonmotor.com](http://www.maxonmotor.com), category «Service & Downloads», Order number 145391.

maxon motor ag    Brünigpass 223    P.O. Box 283    CH-6072 Sachseln    Tel.: +41 (41) 696 15 00    Fax: +41 (41) 696 16 50    www.maxonmotor.com

**maxon motor**

Operating Instructions    4-Q-DC Servoamplifier ADS 50/5

## 2 Performance Data

### 2.1 Electrical data

Supply voltage $V_{CC}$ (Ripple < 5%) .....	12 - 50 VDC
Max. output voltage .....	$0.9 \cdot V_{CC}$
Max. output current $I_{out,max}$ .....	10 A
Continuous output current $I_{out,cont}$ .....	5 A
Switching frequency .....	50 kHz
Efficiency .....	95 %
Band width current controller .....	2.5 kHz
Built-in motor choke .....	150 µH / 5 A

### 2.2 Inputs

Set value .....	-10 ... +10 V ( $R_i = 20 \text{ k}\Omega$ )
Enable .....	+4 ... +50 VDC ( $R_i = 15 \text{ k}\Omega$ )
Input voltage DC tacho "Tacho Input" .....	min. 2 VDC, max. 50 VDC ( $R_i = 14 \text{ k}\Omega$ )
Encoder signals "Channel A, A', B, B'" .....	max. 100 kHz, TTL level

### 2.3 Outputs

Current monitor "Monitor I", short-circuit protected .....	-10 ... +10 VDC ( $R_o = 100 \Omega$ )
Speed monitor "Monitor n", short-circuit protected .....	-10 ... +10 VDC ( $R_o = 100 \Omega$ )
Status reading "READY" .....	max. 30 VDC ( $I_L \leq 20 \text{ mA}$ )

### 2.4 Voltage outputs

Aux. voltage, short-circuit protected .....	+12 VDC, -12 VDC, max. 12 mA ( $R_o = 1 \text{ k}\Omega$ )
Encoder supply voltage .....	+5 VDC, max. 80 mA

### 2.5 Trim potentiometers

IxR compensation	
Offset	
$I_{n,max}$	
gain	

### 2.6 LED indicator

2 coloured LED .....	READY / ERROR
green = ok, red = error	

### 2.7 Ambient temperature- / Humidity range

Operating .....	-10 ... +45°C
Storage .....	-40 ... +85°C
Non condensing .....	20 ... 80 %

### 2.8 Mechanical data

Weight .....	approx. 400 g
Dimensions .....	see dimension drawing
Mounting plate .....	for M4 screws

### 2.9 Terminal

PCB-clamps .....	Power (5 poles), Signal (12 poles)
Pitch .....	3.81 mm
suitable for wire cross section .....	0.14 - 1 mm <sup>2</sup> multiple-stranded wire or
.....	0.14 - 1.5 mm <sup>2</sup> single wire
Encoder .....	Plug DIN41651
	for flat cable, pitch 1.27 mm, AWG 28

**maxon motor**

4-Q-DC Servoamplifier ADS 50/5    Operating Instructions

## 1 Safety Instructions

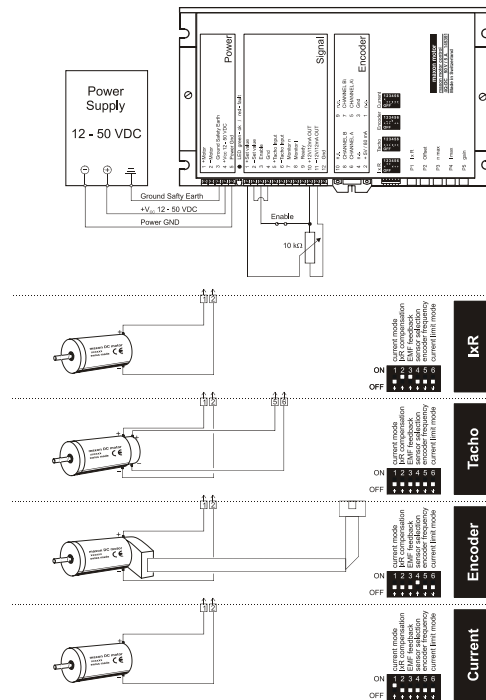
- Skilled Personnel**  
Installation and starting of the equipment shall only be performed by experienced, skilled personnel.
- Statutory Regulations**  
The user must ensure that the servoamplifier and the components belonging to it are assembled and connected according to local statutory regulations.
- Load Disconnected**  
For primary operation the motor should be free running, i.e. with the load disconnected.
- Additional Safety Equipment**  
An electronic apparatus is not fail-safe in principle. Machines and apparatus must therefore be fitted with independent monitoring and safety equipment. If the equipment breaks down, if it is operated incorrectly, if the control unit breaks down or if the cables break, etc., it must be ensured that the drive or the complete apparatus is kept in a safe operating mode.
- Repairs**  
Repairs may be made by authorised personnel only or by the manufacturer. It is dangerous for the user to open the unit or make repairs to it.
- Danger**  
Do ensure that during the installation of the ADS 50/5 no apparatus is connected to the electrical supply. After switching on, do not touch any live parts.
- Max. Supply Voltage**  
Make sure that the supply voltage is between 12 and 50 VDC. Voltages higher than 53 VDC or of wrong polarity will destroy the unit.
- Short circuit and earth fault**  
The ADS 50/5 amplifier is not protected against winding short circuits against ground safety earth or Gnd!
- Motor choke**  
The built in motor choke allows operation with almost all maxon DC motors with an output power higher than 10 Watt. If necessary the motor continuous current must be slightly reduced.  
**Generally the following applies:**  
$$L_{motor} [mH] \geq \frac{V_{CC} [V]}{0.15 \frac{1}{s}} \cdot I_p [mA] - \frac{L_{motor} [mH]}{3}$$
  - Supply voltage  $V_{CC}$  [V]
  - Nominal current (Max. continuous output current)  $I_p$  [mA]
  - Terminal inductance  $L_{motor}$  [mH]**Sought value:**
  - Additional required external inductance so that the continuous current only reduces by max. 10% as a result of warming.

**Electrostatic Sensitive Device (ESD)**

**maxon motor**

4-Q-DC Servoamplifier ADS 50/5    Operating Instructions

## 3 Minimum External Wiring for Different Modes of Operation





## 4 Operating Instructions

### 4.1 Determine power supply requirements

You may make use of any available power supply, as long as it meets the minimal requirements spelled out below.  
During set up and adjustment phases, we recommend separating the motor mechanically from the machine to prevent damage due to uncontrolled motion.

Power supply requirements

Output voltage	VCC min. 12 VDC; max. 50 VDC
Ripple	< 5 %
Output current	depending on load, continuous 5 A (short-time 10 A)

The required voltage can be calculated as follows:

#### Known values

- ⇒ Operating torque  $M_B$  [mNm]
- ⇒ Operating speed  $n_B$  [rpm]
- ⇒ Nominal motor voltage  $U_N$  [Volt]
- ⇒ Motor no-load speed at  $U_N$ ,  $n_0$  [rpm]
- ⇒ Speed/torque gradient of the motor  $\Delta n/\Delta M$  [rpm/mNm]

#### Sought values

- ⇒ Supply voltage  $V_{CC}$  [Volt]

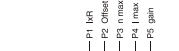
$$V_{CC} = \frac{U_N}{n_0} \left( n_B + \frac{\Delta n}{\Delta M} \cdot M_B \right) \cdot \frac{1}{0.9} + 2 [V]$$

Choose a power supply capable of supplying this calculated voltage under load. The formula takes into account a max. PWM cycle of 90 % and a 2 volt max. voltage drop.

#### Consider

The power supply must be able to buffer the back-fed energy from brake operation e.g. in a condenser. With electronically stabilized power supply units it is to ensure, that the overcurrent protection responds in no operating condition.

### 4.2 Function of the potentiometers



Potentiometer	Function	left	Turn to the right
P1	IxR compensation	weak compensation	strong compensation
P2	Offset	Adjustment $n = 0 / I = 0$ at set value 0 V	motor turns CCW / motor turns CW
P3	$n_{max}$ at 10 V set value	max. speed slower	speed faster
P4	$I_{max}$	current limit lower min. 0.5 A	higher max. 10 A
P5	gain	amplification lower	higher

## 5 Functions

### 5.1 Inputs

#### 5.1.1 Set value

The set value input is wired as a differential amplifier.

Input voltage range	-10 ... +10 V
Input circuit	differential
Input resistance	20 kΩ (differential)
Positive set value	(+ Set value) > (- Set Value) negative motor voltage or current motor shaft turns CCW
Negative set value	(+ Set value) < (- Set Value) positive motor voltage or current motor shaft turns CW

#### 5.1.2 Enable

If a voltage is given at "Enable", the servoamplifier switches the motor voltage to the winding connections. If the "Enable" input is not switched on or is connected to the Gnd, the power stage will be highly resistant and will be disabled. The "Enable" input is short-circuit protected.

Enable	Minimum input voltage	+ 4.0 VDC
	Maximum input voltage	+ 50 VDC
	Input resistance	15 kΩ
	Switching time	typ 500 μs (by 5 V)
Disable	Minimum input voltage	0 VDC
	Maximum input voltage	+ 2.5 VDC
	Input resistance	15 kΩ
	Switching time	typ 100 μs (by 0 V)

#### 5.1.3 DC Tacho

Minimum input voltage	2.0 V
Maximum input voltage	50 V
Input resistance	14 kΩ

#### Speed control range:

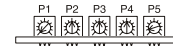
The speed range is set using Potentiometer P3  $n_{max}$  (max. speed at maximum set value).  
For full speed control with  $\pm 10$  V, the tacho input voltage range must be at least  $\pm 2$  V.

Example for DC-Tacho with 0.52 V / 1000 rpm:  
2.0 V tacho voltage is equivalent to a speed of approx. 3850 rpm. If the full set value range has been used, the lowest adjustable speed with the  $n_{max}$  potentiometer is 3850 rpm.  
Lower speed ranges can be reached through a reduced set value range or by using a DC tacho with a higher output voltage, such as 5 V / 1000 rpm.

## 4.3 Adjustment of the Potentiometers

### 4.3.1 Pre-adjustment

With the pre-adjustment, the potentiometers are set in a preferred position. ADS units in original packing are already pre-adjusted.



Pre-adjustment of potentiometers		
P1	IxR	0 %
P2	Offset	50 %
P3	$n_{max}$	50 %
P4	$I_{max}$	50 %
P5	gain	10 %

### 4.3.2 Adjustment

#### Encoder mode DC-Tacho mode IxR compensation

- Adjust set value to maximum (e.g. 10 V) and turn potentiometer P3  $n_{max}$  so far that the required speed is achieved.
- Set potentiometer P4  $I_{max}$  at the limiting value desired. Maximum current in the 0 ... 10 A range can be adjusted in linear fashion with potentiometer P4. Important: The limiting value  $I_{max}$  should be below the nominal current (max. continuous current) as shown on the motor data sheet and may not exceed 5 A continuously.
- Increase potentiometer P5 gain slowly until the amplification is set large enough. Caution: If the motor vibrates or becomes loud, the amplification is adjusted too high.
- Adjust set value to 0 V, e.g. by short circuiting the set value. Then set the motor speed to 0 rpm with the potentiometer P2 Offset. In addition, only in the case of IxR compensation:
- Slowly increase potentiometer P1 IxR until the compensation is set large enough so that in the case of high motor load the motor speed remains the same or decreases only slightly. Caution: If the motor vibrates or becomes loud, the amplification is adjusted too high.

#### Current controller mode

- Set potentiometer P4  $I_{max}$  at the limiting value desired. Maximum current in the 0 ... 10 A range can be adjusted in linear fashion with potentiometer P4. Important: The limiting value  $I_{max}$  should be below the nominal current (max. continuous current) as shown in the motor data sheet and may not exceed 5 A continuously.
- Adjust set value to 0 V. Then set the motor current to 0 A with the potentiometer P2 Offset.

#### Note

- A set value in the -10 ... +10 V range is equal to a current range of approx.  $+I_{max}$  ...  $-I_{max}$
- Configured as a current controller, P1, P3 and P5 are not activated.

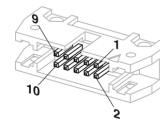
### 5.1.4 Encoder

Encoder supply voltage	+ 5 VDC max. 80 mA
Maximum encoder frequency	DIP switch S5 ON: 10 kHz
	DIP switch S5 OFF: 100 kHz
Voltage value	TTL low max. 0.8 V
	high min. 2.0 V

It is strongly recommended that the encoder be used with a built-in line driver. If the encoder is used without a line driver (without CHA and CHB), speed breakdowns and max. speed limits must be expected because of the slower switching slope.

The servoamplifier does not need any home impulse I and II.

#### Male header (front view)



#### Pin configuration at "Encoder" input:

1	n.c.	Not connected
2	+5 V	+ 5 VDC max. 80 mA
3	Gnd	Ground
4	n.c.	Not connected
5	A1	Inverted Channel A
6	A	Channel A
7	B1	Inverted Channel B
8	B	Channel B
9	n.c.	Not connected
10	n.c.	Not connected

This pin configuration is compatible with the flat cable plugs in Encoder HEDL 55xx (with Linedriver) and the MR encoders with line driver, type ML and L.

## 5.2 Outputs

### 5.2.1 Current monitor "Monitor I"

The servoamplifier makes a current actual value available for monitoring purposes. The signal is proportional to the motor current. The "Monitor I" output is short-circuit protected.

Output voltage range	-10 ... +10 VDC
Output resistance	100 Ω
Gradient	approx. 0.8 V/A
positive voltage on current monitor output	corresponds to a negative motor current
negative voltage on current monitor output	corresponds to a positive motor current

### 5.2.2 Speed monitor "Monitor n"

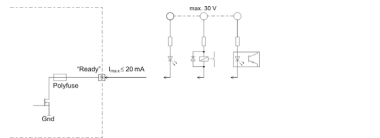
The speed monitor is primarily intended for the qualitative estimation of the dynamics. The absolute speed is determined by the properties of the speed sensors and by the setting of the  $n_{max}$  potentiometer. The output voltage of the speed monitor is proportional to the number of revolutions. The output voltage of the speed monitor is 10 V when the maximum number of revolutions set by the  $n_{max}$  potentiometer has been reached. The "Monitor n" output is short-circuit protected.

Output voltage range	-10 ... +10 VDC
Output resistance	100 Ω

Example: -10 V corresponding speed  $-n_{max}$  (CCW)  
 0 V corresponding speed 0 rpm  
 +10 V corresponding speed  $+n_{max}$  (CW)

### 5.2.3 Status reading "Ready"

The "Ready" signal can be used to report the state of operational readiness or a fault condition on a master control unit. The "Open Collector" output is, in normal cases, i.e., no faults, switched to Gnd. In the case of a fault due to excess temperature, excess current, voltage processing error or too high encoder input frequency, the output transistor is disabled.



An external additional voltage is required:

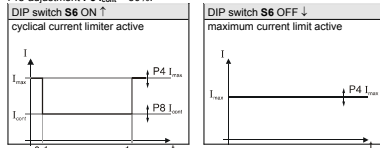
Input voltage range	max. 30 VDC
Load current	≤ 20 mA

The fault condition is stored. In order to reset the fault condition, the servoamplifier must be re-released (Enable). If the cause of the fault situation cannot be removed, the output transistor will immediately change to the not conducting state again.

## 6.2 Adjustments potentiometer P8 $I_{cont}$ and current limit mode DIP switch S6

It is standard that a maximum current limiter is activated (DIP switch S6 OFF). In this way the motor current is limited to the value set on potentiometer P4  $I_{max}$  (0.5 ... 10 A). If DIP switch S6 is turned to ON, a cyclical current limiter is also activated. This current limiter method makes a certain level of motor protection against thermal overload possible. For 0.1 seconds the motor current is limited to the value set on potentiometer P4  $I_{max}$  (0.5 ... 10 A) and then for 0.9 seconds current is limited to the value set on potentiometer P8  $I_{cont}$  (0.5 ... 10 A). After one second the cycle will repeat itself.

Pre-adjustment P8  $I_{cont}$  = 50%.



## 6.3 Maximal encoder frequency DIP switch S5

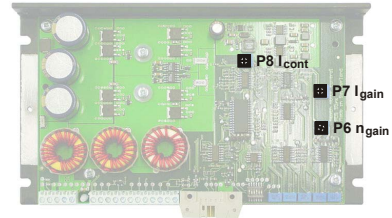
DIP switch S5 permits selection of the maximum encoder input frequency. A max. encoder frequency of 100 kHz is standard.

DIP switch S5 ON ↑ Max. input frequency is 10 kHz		DIP switch S5 OFF ↓ Max. input frequency is 100 kHz	
Encoder pulse per turn	maximum motor speed	Encoder pulse per turn	maximum motor speed
16	37 500 rpm		
32	18 750 rpm		
64	9 375 rpm		
128	4 688 rpm	128	46 875 rpm
256	2 344 rpm	256	23 438 rpm
500	1 200 rpm	500	12 000 rpm
512	1 721 rpm	512	11 719 rpm
1000	600 rpm	1000	6 000 rpm
1024	586 rpm	1024	5 859 rpm

**Note**  
 To achieve good control characteristics, encoders with low impulse counts per turn should be run with the DIP switch S5 ON ↑.

## 6 Additional Possible Adjustments

Potentiometer	Function	Position	left	right
P6 $n_{gain}$	speed gain		low	high
P7 $I_{gain}$	current gain		low	high
P8 $I_{cont}$	continuous current limit		lower	higher



## 6.1 Adjustments potentiometer P6 $n_{gain}$ and potentiometer P7 $I_{gain}$

In most applications, regulation setting is completely satisfactory using potentiometers P1 to P5. In special cases the transient response can be optimized by setting the P6 "speed regulation gain" potentiometer. The P7 "current regulator gain" potentiometer can, in addition, be adapted to the dynamics of the current regulator.

It is recommended that the success of changes to the settings of P6  $n_{gain}$  and P7  $I_{gain}$  be checked by measuring the transient response with an oscilloscope at the "Monitor n" and "Monitor I" outputs.

Pre-adjustment P6  $n_{gain}$  = 25 % and P7  $I_{gain}$  = 40 %.

## 7 Operating Status Display

A two coloured red/green LED shows the operating mode.

### 7.1 No LED

Reason:

- No supply voltage
- Fuse fault
- Wrong polarity of supply voltage
- Short circuit of the +5 V output

### 7.2 LED shines green

Blink pattern (green LED)	Operating Conditions
LED on	Amplifier is activated (Enable)
[Blinking pattern]	Disable function active

### 7.3 LED shines red

According to the blink pattern the following error messages can be identified:

Blink pattern (red LED)	Operating Conditions
① [Blinking pattern]	If the power stage temperature exceeds a limit of approx. 90 °C, the power stage is switched off (disable status).
② [Blinking pattern]	If a motor current of more than approx. +/- 12.5 A is detected at the current actual value, the power stage will be switched off (disable status). If the internal supply voltage cannot be set-up as expected the power amplifier is switched off (disable status).
③ [Blinking pattern]	If the input frequency at the encoder input is > 150 kHz, expected the power amplifier is switched off.
④ [Blinking pattern]	

The fault condition is stored. In order to reset the fault condition, the servoamplifier must be re-released (Enable). If the cause of the fault condition cannot be eliminated, the error output will be disabled again immediately.

Reason:

- High ambient temperature (blink pattern ①)
- max. continuous current > 5 A (blink pattern ②)
- bad convection (blink pattern ③)
- Short circuit on the motor winding (blink pattern ④)

## 8 Error Handling

Defect	Possible source of defect	Measures
Shaft does not rotate	Supply voltage < 12 VDC	check power plug pin 4
	Enable not activated	check signal plug pin 3
	Set value is 0 V	check signal plug pin 1 and pin 2
	Current limit too low	check adjustment potentiometer <b>P4</b> $I_{max}$
	Wrong operational mode	check DIP switch settings
Speed is not controlled	Bad contacts	check wiring
	Wrong wiring	check wiring
	Encoder mode: encoder signals	check plug encoder
DC-Tacho mode: tacho signals	check plug signal pin 5 and 6 (polarity)	
ixR mode: compensation wrong	check adjustment potentiometer <b>P1</b>	

## 9 EMC-compliant installation

- Power supply (+V<sub>cc</sub> - Power Gnd)**
- No shielding normally required.
  - Star point-shaped wiring if several amplifiers are supplied by the same power supply.

**Motor cable**

- Shielded cable highly recommended.
- Connect shielding on both sides:  
ADS 50/5 side: Terminal 3 "Ground Safety Earth" and/or bottom of housing.  
Motor side: Motor housing or with motor housing mechanical design with low resistive connection.
- Use separate cable.

**Encoder cable**

- Although the ADS 50/5 can also be operated without a line driver, using an encoder with a line driver is recommended as this improves interference resistance.
- No shielding normally required.
- Use separate cable.

**Analogue signals (Set value, Tacho, Monitor)**

- No shielding normally required.
- Use cable shielding with analogue signals with small signal level and electromagnetically harsh environment.
- Normally connect shielding on both sides. Place shielding on one side if there are 50/60 Hz interference problems.

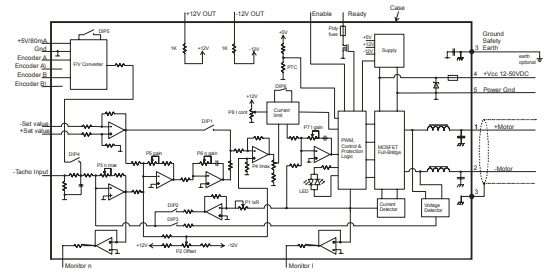
**Digital signals (Enable, Ready)**

- No shielding necessary.

See also block diagram in chapter 10.

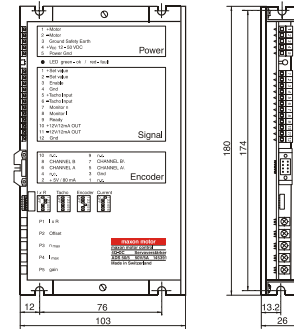
In practical terms, only the complete equipment, comprising all individual components (motor, amplifier, power supply unit, EMC filter, cabling etc.) can undergo an EMC test to ensure interference-free CE-approved operation.

## 10 Block Diagram



## 11 Dimension Drawing

Dimensions in [mm]



## F Measurements with the new actuator

### F.1 Without Flat Plank

Table 7: The voltage sent from the laptop to the TUEdACS with the corresponding velocity of the actuator

Voltage [V]	Velocity [V/s]
-4.0000	-0.1748
-2.0000	-0.1752
-1.0000	-0.0857
-0.5000	-0.0417
0.5000	0.0397
1.0000	0.0828
2.0000	0.1670
4.0000	0.1659

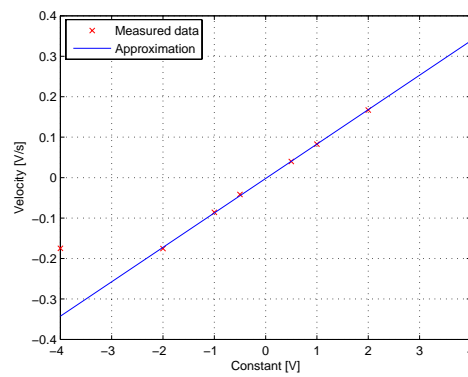


Figure 31: The input voltage plotted against the velocity of the actuator

Figure 31 is obtained from the data in table 7. From this, it follows that the relation between the output voltage of the laptop and the velocity of the actuator is described best by

$$\dot{d}_v = 0.0851 \cdot V_L - 0.0022 \quad (15)$$

Figure 32 shows the response of the actuator for three different sine waves.

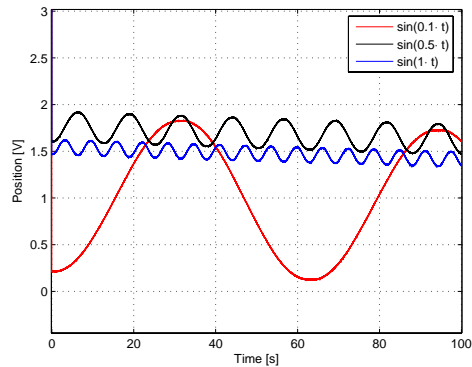


Figure 32: Three sine waves

## F.2 On the plank

Table 8: The output voltage of the laptop with corresponding velocities of the actuator and the angular velocity of the plank, obtained from the knowing that  $1 \text{ V} \equiv 25.48 \text{ mm}$  (section 5.1) and the calibration in appendix G

Voltage [V]	Velocity [V/s]	Velocity [mm/s]	Velocity [ $^{\circ}$ /s]
0.4	0	0	0
0.5	0	0	0
0.6	0.0116743	0.29751	-0.0953873
0.7	0.0178372	0.454568	-0.145743
0.8	0.0272572	0.694628	-0.222711
0.9	0.0362934	0.924907	-0.296542
1	0.0466912	1.18989	-0.3815
1.2	0.0541697	1.38047	-0.442604
1.4	0.0688999	1.75586	-0.56296
1.6	0.104915	2.67367	-0.857226
1.8	0.122097	3.11155	-0.99762
2	0.142382	3.62848	-1.16336
2.2	0.157607	4.01649	-1.28776
2.4	0.178305	4.54395	-1.45687
2.6	0.191321	4.87567	-1.56323
2.8	0.205672	5.24139	-1.68049
3	0.202914	5.17109	-1.65795
3.2	0.203646	5.18976	-1.66393
3.4	0.204693	5.21644	-1.67249
3.6	0.204401	5.20898	-1.6701
3.8	0.204559	5.21302	-1.67139
4	0.205895	5.24707	-1.68231
4.2	0.204617	5.2145	-1.67186
4.4	0.207983	5.30028	-1.69937
4.6	0.205066	5.22595	-1.67554
4.8	0.202226	5.15357	-1.65233
5	0.203818	5.19414	-1.66534
5.2	0.205699	5.24209	-1.68071

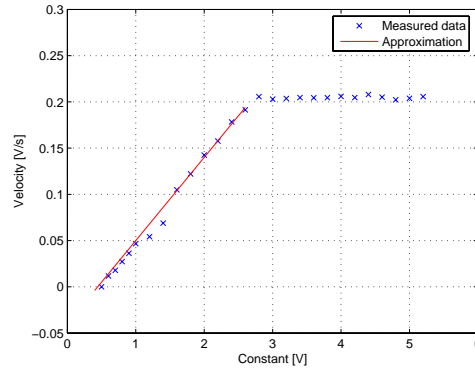


Figure 33: The input voltage plotted against the velocity of the actuator

Figure 33 is obtained from the data in table 8. From this, it follows that the relation between the output voltage of the laptop and the velocity of the actuator best is described by

$$\dot{d}_v = 0.09 \cdot V_L - 0.04 \quad (16)$$

and

$$\dot{\delta} = -0.75 \cdot V_L + 0.35 \quad (17)$$

Following from the table, the maximum absolute angular velocity of the plank is  $1.68 \text{ }^\circ/\text{s}$ . The angular velocities being negative, is due to the definition of the sign of the angle, see appendix G. With

$$\delta = A \cdot \sin(\omega \cdot t) \quad (18)$$

and

$$\dot{\delta} = A \cdot \omega \cdot \cos(\omega \cdot t) \quad (19)$$

the limit sine waves are  $15 \cdot \sin(0.112 \cdot t)$  and  $1 \cdot \sin(1.68 \cdot t)$ .

Figure 34 shows the response of the actuator on three different sine waves.

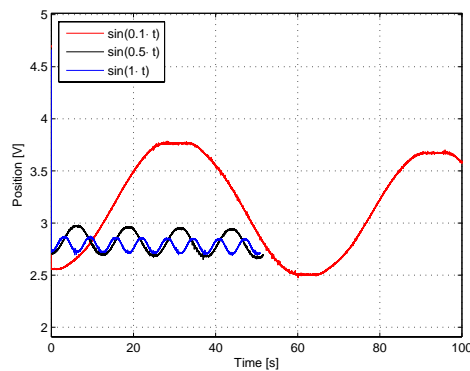


Figure 34: Three sine waves

When the response of the actuator on both the constant voltages and the sine waves without and with plank are compared, it is clear that the maximum velocity of the actuator is higher for the latter situation, namely  $0.167 \text{ V/s}$  resp.  $0.207 \text{ V/s}$ , but that it does take a higher voltage to reach the same

velocity. Also, the actuator starts to move in the first situation at an input of 0.5 V, while the actuator needs a minimum input of 0.6 V in the second situation. Furthermore, the amplitude of the sine waves are in the latter case lower than in the former. From this, the conclusion that a feedback control is needed is drawn.

## G Calibration of the actuator

A calibration measurement with the actuator at the Flat Plank is done to know the relation between the output voltage of the actuator and the angle of the plank. For about every half angle between  $-15$  and  $15^\circ$  the output voltage has been measured. This leads to the following values:

Table 9: The angle of the plank with corresponding output voltage

Angle [ $^\circ$ ]	Voltage [V]	Angle [ $^\circ$ ]	Voltage [V]
15.2	0.079	-0.4	2.092
15.1	0.139	-1.0	2.170
15.0	0.185	-1.5	2.232
14.5	0.293	-2.0	2.290
13.9	0.377	-2.7	2.374
12.9	0.491	-3.0	2.417
12.0	0.597	-3.5	2.473
11.4	0.673	-4.1	2.547
11.0	0.717	-4.5	2.599
10.5	0.778	-5.0	2.664
9.9	0.843	-5.6	2.73
9.4	0.906	-5.9	2.751
8.95	0.954	-6.7	2.864
8.4	1.022	-7.2	2.924
7.95	1.079	-7.5	2.967
7.4	1.144	-7.9	3.021
6.9	1.199	-8.4	3.080
6.4	1.257	-9.3	3.187
5.9	1.323	-9.9	3.266
5.2	1.412	-10.5	3.341
4.9	1.455	-11.1	3.414
4.4	1.507	-11.7	3.488
3.9	1.5665	-12.1	3.533
3.4	1.633	-12.6	3.597
2.9	1.684	-13.1	3.661
2.4	1.7545	-13.5	3.713
1.9	1.812	-14.2	3.794
1.3	1.882	-14.4	3.831
0.9	1.928	-15.5	3.950
0.3	2.000	-16.1	4.040
		-16.4	4.160



From this table, the following graph can be drawn. From this, the relation between the voltage and

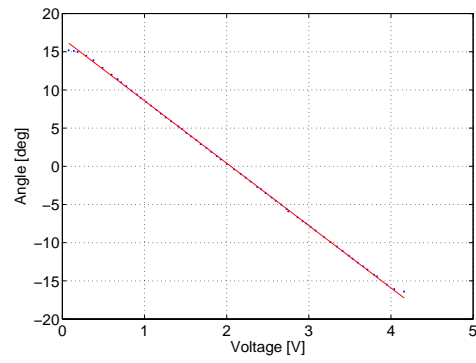


Figure 35: The feedback voltage of the actuator vs. the angle of the plank  
the angle of the plank appeared to be

$$\delta = -8.1707 \cdot V + 16.7579 \quad (20)$$

## H Frequency response

Table 10: Frequencies of the sine input signal and the resulting amplitude and phase lag of the actuator

Frequency [rad/s]	Amplitude [V]	Phase [rad]
0.08	0.7602	1.44
0.1	0.6827	1.2
0.2	0.3673	1.6
0.5	0.15	1.5
0.6	0.1391	1.3
0.8	0.1	1.6
1	0.0919	1.9
2	0.0537	1.9
5	0.015	1.75
10	0.007	2



## References

- [1] Hans B Pacejka, *Tyre and vehicle dynamics*, Butterworth-Heinemann, Oxford, United Kingdom, 2002
- [2] R.T. Uil, *Non-lagging effect of motorcycle tyres. An experimental study with the Flat Plank Tyre Tester*, internal report, Eindhoven University of Technology, The Netherlands, 2006
- [3] Vittore Cossalter, *Motorcycle tyre research results*, University of Padova, Padova, Italy, 2006